THE CREATION OF WOVEN TILES FROM THE UNION OF DELAUNAY LOFTS

A Thesis

by

MATTHEW R. ENG

Submitted to the Office of Graduate and Professional Studies of
Texas A&M University
in partial fulfillment of the requirements for the degree of

MASTER OF SCIENCE

Chair of Committee,	Ergun Akleman
Committee Members,	Vinayak Krishnamurthy
	Richard Davison
	Alan Freed
Head of Department,	Tim McLaughlin

December 2019

Major Subject: Visualization

ABSTRACT

In this work, we build upon the previously established foundations of Delaunay Lofts, which are a new class of shapes inspired by biological phenomena known as scutoids. Delaunay Lofts naturally provides edge collapse and vertex split processes, which make them highly complex in terms of topological structure. Delaunay lofts are obtained by layer-by-layer Voronoi decomposition of points. Therefore, any cross-section of a Delaunay Loft is always a convex polygon. Moreover, the only topology change from one layer to another is the change in the number of sides of cross-section polygons.

Through our methodology, we obtain woven tiles as the union of Delaunay Lofts. This extension provides two advantages over the original Delaunay Lofts that can lead to woven tiles: (1) Each cross-section polygon can be non-convex, and (2) we can connect and disconnect polygons. To create woven tiles, we use unions of a linear pattern of points that can produce patterns similar to woven textiles. We have only investigated two widely used woven patterns: plain and twill. Plain woven tiles provide an approach to construct generalized Abeille's flat vaults, which was introduced by French engineer and architect Joseph Abeille. Twill patterns provide even further generalizations of Abeille's vaults, thus demonstrating the existence of a general class of woven tiles.

By taking the union of several individual Delaunay Lofts, woven tiles appear in the resulting structure. Using this method, we are able to create non-convex polygons, as well as connecting and disconnecting the polygons in any manner we desire. Additionally, we can design the resulting shapes on each layer since we have control of the Voronoi Site locations. In developing this approach, we created a procedural framework that allows for the manipulation of rules and guidelines for the creation of the Delaunay Loft. As a result, we are able to generate a wide variety of Woven Structures based on Delaunay Lofts from tweaking various parameters. Using this method, we 3D printed some Woven Structures in order to help analyze symmetrical, structural, and tiling

properties.

DEDICATION

To my family and friends.

ACKNOWLEDGMENTS

I would like to acknowledge and thank my committee chair, Dr. Ergun Akleman, for his relentless assistance, support, and guidance on this project. Not only was it an honor to push the boundaries of geometric shape modeling with him, but I know I learned a lot of wisdom from him outside of the classroom.

I would also like to recognize the support from my co-chair, Dr. Vinayak Krishnamurthy. His serious work ethnic and dedication to academia was inspiring and helped me persevere throughout this project.

I would also like to thank my colleague, Sai Ganesh Subramanian for his help. I appreciate the camaraderie while working together during those late nights to meet those deadlines set by Ergun and Vinayak.

I would also like to thank the rest of my committee, Richard Davison and Alan Freed, for their support.

I would also like to thank my family and friends for all of their unwavering love, support, and encouragement. I couldn't have completed this journey without them.

CONTRIBUTORS AND FUNDING SOURCES

Contributors

This work was supervised by a thesis committee consisting of Professor Ergun Akleman and Richard Davidson from the Department of Visualization. Professor Vinayak Krishnamurthy and Alan Freed were also involved from the Department of Engineering.

Additionally, Sai Ganesh Subramanian, a student from the Department of Engineering, was involved early on in setting the foundation for our previous research about Delaunay Lofts. We collaborated together successfully as colleagues to implement our algorithm in two separate software packages yielding similar results.

All work conducted for the thesis was completed by the student independently.

Funding Sources

There are no outside funding contributions to acknowledge related to the research and compilation of this document.

TABLE OF CONTENTS

Page

LIST OF FIGURES

FIGURE Page

1. INTRODUCTION AND MOTIVATION

Throughout history, architects have experimented with structural forms that were innovative while maintaining aesthetic integrity. Basic bricks (or rectangular blocks) are within the family of regular prisms, which are simple to manufacture and easily accessible. However, an over reliance on regular prisms severely limits the design for obtaining other structures, which can potentially be even more dependable while even more visually fascinating [50, 13, 51, 44, 34]. Currently, architects are searching for other space filling elements, but their processes are usually not systematic and are limited to the building blocks they investigate [16]. Therefore, there arises a need for conceptualizing approaches that enables the design and control of a wide variety of modular and tileable building elements.

In terms of energy consumption in developed countries, the global contribution from both residential and commercial buildings has increased to figures between 20% - 40%, which bypassed other sectors such as industrial and transportation [38]. Therefore, there is a need to direct efforts towards discovering opportunities that will help buildings reduce their energy consumption. Non-woven fabrics are materials made up of fibres that are bonded together through chemical and mechanical treatment, and have been around since the 1930's. Various patents [5, 39, 10, 22, 14, 2] have focused on the engineering to construct non-woven textile structures. As a result of comparative analysis of non-woven fabrics [6, 40], non-woven fabrics have steadily been replacing woven materials in many industrial applications ranging from engineering to medicine as they provide more ideal behavior and reliability [11, 4]. However, these findings are not meant to discount the potential of woven fabrics. Grunbaum and Shephard were the first to formally investigate the mathematics behind 2-way, 2-fold woven fabrics - such as the plain, twill, and satin patterns [26]. An important concept that the pair introduced was the idea of "hang-together" or "fall-apart". If the fabric is woven, certain patterns are considered to fall-apart if some interlaced warp and weft threads are not completely interlaced with the rest of the fabric. As a result, such a fabric would come apart in pieces. Conversely, woven patterns that hang-together keep their layout integrity

and are therefore self-supporting. This important characteristic can be desirable when considering static loading or structural equilibrium.

Groundbreaking work occurred recently in the biological community through the discovery of "scutoids" — shapes that frequently occur in epithelial cells [21]. Previously, the cells were thought to pack together in order to reduce the amount of surface energy by forming in prism-like shapes. Epithelial cells typically cover the surface of several human organs, allowing them to curve, bend, and fold as they form and develop into various shapes. As the cell layers grow, each individual cells adapts its shape in accordance with the whole organ, as efficiently as possible. Now, the scutoid structures are shown to display a topology change through edge-collapse and vertex-split operations between quadrilateral, pentagonal, and hexagonal faces of any tessellation.

2. BACKGROUND AND LITERATURE REVIEW

2.1 Architecture

Joseph Abeille was a French engineer and architect whose work includes his designs for the Lullin Hotel, Thunstetten Castle, and various projects centered around canal/hydraulic applications. However, his most noted contribution in the field of architecture may be his flat vault - an interlocking woven-like design pattern used for structural applications in covering a space.

Researchers have investigated the importance of the Abeille Flat Vault's interlocking properties in terms of geometric constraints as an application towards non-planar assemblies [37]. The results indicate that Abeille-like structures demonstrate potential understanding for how geometric relationships help interact within an overall assembly, and how individual elements help handle "the transfer of structural principles between different construction typologies which in turn helps to delimit system boundaries and opens up the possibility of a more fluid understanding of structures in architecture" [37].

Stereotomy is the art and science of cutting three-dimensional solids into particular shapes. During the process, materials are cut and assembled into complex shapes. Miadragovivc applied this process to Abeille's Flat Vault to discover its' limits for construction purposes [36]. This helps provide an understanding of the composition of the entire structural capacity of an entire system based on its individual elements.

2.2 Tilable and Space Filling Shapes

A space filling shape is one that, when replicated and repeated, can completely fill a given space - that is, without having any voids between elements [35]. As an extension of this, a space filling shape is therefore a structure that is tileable so as to form a tessellation in a given space [30].

A prominently known example is the cube, which is the only space filling Platonic solid [17]. Further investigation into space filling polyhedia, or polygons "whose replications can be packed to fill three-space completely" was conducted by Goldberg [18, 19, 20]. Work by Williams found

that further examples of space-filling polyhedra were related to occurrences in nature through soap bubbles and plant cells, and that even some of them had regular faces [52, 53]. Furthermore, the Johnson solid gyrobifastigium provided evidence of convex polyhedra that was even linked to molecular structure in chemistry applications [32, 3].

As fabrication technology has improved in terms of precision and cost effectiveness, as well as advancement in materials science, there has been a growing interest in the mechanical characterization of 3D printed 2D tilings in the context of "sheet materials"[43]. Within this scenario, the sheet material can be seen as a thin extrusion of a 2D tiling. Kaplan and Rao demonstrate two interesting cases of designing 2D tilings - Kaplan uses artistic patterns by carefully selecting the position of Voronoi Site locations [33] and Rao uses a systematic approach to generate 2D pentagonal tilings [41].

2.3 Woven Structures

In addition to classifying woven structures as hang-together or fall-apart, Grunbaum and Shephard also coined the word, isonemal fabrics, to describe fabrics that have a transitive symmetry group on the strands of the fabric [29]. They also provided images of all non-twill isonemal fabrics (i.e. hanging-together weaves) of periods up to 17 [27, 28]. As a result, other researchers began to develop algorithms to determine whether or not a fabric is considered to hang-together [25, 8, 9, 15, 12]. Furthermore, other researchers such as Roth [42], Thomas [49, 48, 47], Zelinka [54, 55], and Griswold [23, 24] primarily studied the theoretical and practical symmetry properties of isonemal fabrics, as well as other properties. Chen et al. expressed an alternative notation, [a, b, s], to express patterns because it is useful to show the initial row pattern, with fall-apart and hang-together being easily identifiable if the combination of variables are relatively prime or not [7].

2.4 Biology

Previous research determined that in skin cells, the top (apical) and bottom (basal) surfaces of the cellular structure are Voronoi patterns (as these occur frequently due to physical con-

straints) [31]. Research led by Gómez-Gálvez et al.[21], observed that simple polyhedral form, called "scutoids", that commonly exist in epithelial cells in the formation of skin cells. Inspired by this newly discovered scutoid shape, work by Subramanian et.al introduced an approach to "design a new class of tilings in 3D space" by taking the "Voronoi tessellations based on some distribution of points" on a plane and then interpolating the tilings between several planes called Delaunay Lofts. [46]. The work established an algorithm that was driven by controlling the Voronoi Sites as input in order to generate a series of complex shapes. Interestingly, the scutoid was a natural result of their Delaunay Loft algorithm. Initial mechanical strength tests provided through FEA (Finite Element Analysis) provide evidence that suggests Delaunay Lofts carry characteristics that are ideal from a structural perspective as "the stress distribution decreases around the critical points where the topology changes." [46]. As an extension of this work, using focused knowledge about designing the Voronoi Site points could potentially lead to mechanically superior designed shapes.

2.5 Putting it All Together

We seek to accomplish this by proposing an approach and algorithm that expands on Delaunay Lofts by harnessing the power of specific Voronoi site configurations in order to generate mechanically capable structures that are inspired and exhibit geometric symmetry by the woven structure patterns based on Joseph Abeille's flat vault.

3. PROCESS

3.1 Introduction

In this chapter, we provide the basic steps of our process that is used to develop several Delaunay Lofts. Our process consists of the following 8 steps as described in this chapter.

1. Establishment of a 3D Domain for Designing Woven Tiles
2. Creation of Control Lines
3. Sampling the Control Lines
4. Creation of Control Curves
5. Subdivision of each Layer into Convex Polygons Using Voronoi Decomposition
6. Constructing Non-convex or Disconnected 2D as the Union of Convex Voronoi Polygons
7. Obtain Extruded Polygons
8. Union of Extruded Voronoi polygons

In the rest of this chapter, we provide details of each step.

3.2 Establishment of a 3D Domain for Designing Woven Tiles

We start with a volumetric cubic domain $S = x, y, z|max(x, y, z) < 1$. The initial step of our process is to provide a 2D square domain $S = x, z|max(x, z) < 1$ with a rectangular grid consisting of N number of columns and rows as shown in Figure 3.1a. We make M copies of this 2D square domain along y starting from $y = 1$ to $y = -1$. We call the two 2D square domains with associated rectangular grids in the planes $y = 1$ and $y = -1$“, the Top and Bottom Layers”, as shown in Figure 3.1b. This process provides a stack of layers along the y-axis, considered as the height, as shown in Figure3.1c. The grid associated with each 2D square domain is used to model

the corresponding patterns of 2-way, 2-fold fabrics in the top and bottom layers [1]. Our goal is to obtain tiles that can logically connect 2-way, 2-fold fabric patterns in the top and bottom layers. Intermediate layers are used between the top and bottom layers in order to compute the shape of woven tiles.

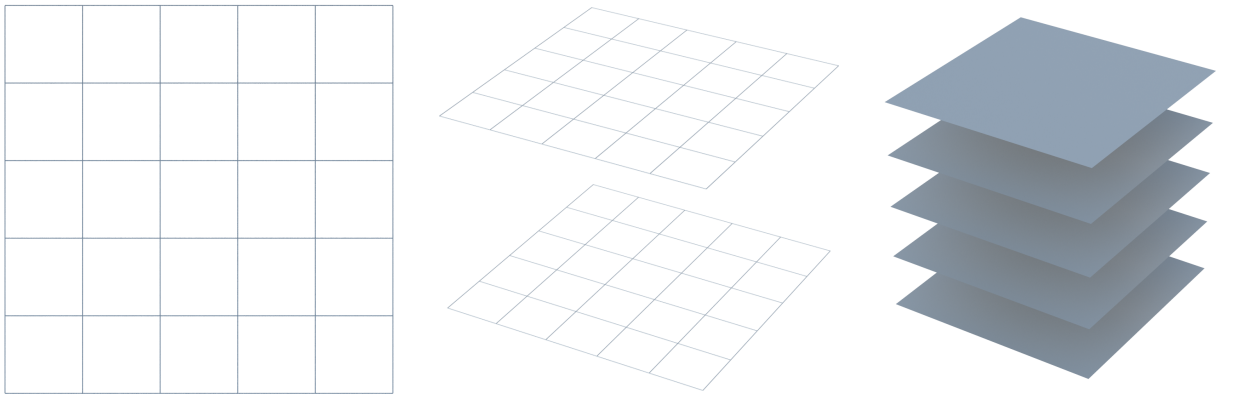

(a) Defining the 2D Grid Space.

(b) Visualizing the Top and Bottom Grid Layers Only.

(c) Visualizing Grids Stacked on top of each other as Layers.

Figure 3.1: Step 1: Establishment of a 3D Domain for Designing Woven Tiles.

3.3 Creation of Control Lines

The second step is to construct the corresponding woven patterns of 2-way, 2-fold fabrics in the top and bottom layers. The woven patterns in our case are described as lines closed under a set of symmetry operations [27]. This process can create lines that are laid out in a formation that correspond to a specific 2-way, 2-fold Fabric pattern. For instance, Figure 3.2 shows a formation that corresponds to the plain weaving pattern. The top layer is shown in Figure 3.2 (a), and the bottom layer is shown in Figure 3.2 (b). We use the lines as controls in order to create guides for the position of Voronoi Sites. Therefore, we call these lines as control lines.

3.4 Sampling the Control Lines

The third step is to sample each control line with a set of points that are used as Voronoi Sites. This sampling process is mainly used to direct control of the Voronoi polygon shapes. As we

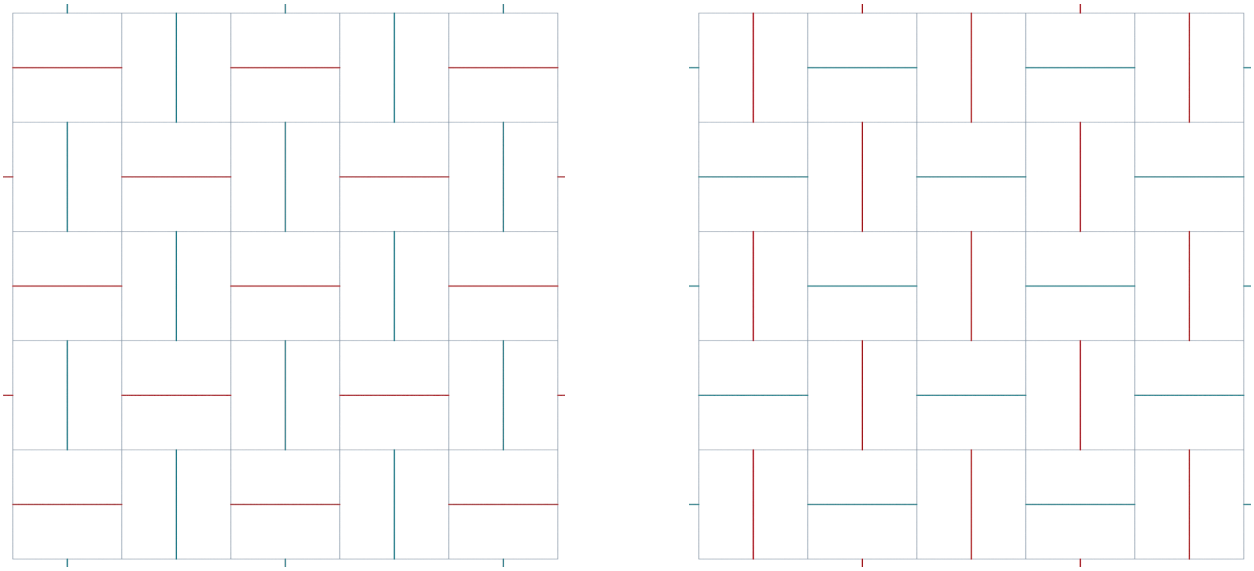

(a) Plain Weave Pattern Applied to the Top Layer.

(b) Plain Weave Pattern Applied to the Bottom Layer.

Figure 3.2: Step 2: An example of control line creation whose formation correspond to the plain woven patterns at the top and bottom layers.

demonstrate in Chapter 5, both the number and distribution of Voronoi points on each control line effects the geometry and topology of polygons in each layer. In other words, sampling is essential to control the final shapes of Woven tiles.

Figure 3.3 shows examples of sampling uniformly distributed points on each of the control lines at the top layer for the plain weave pattern. Figure 3.3 provides 3, 5, 10 and 20 uniformly sampled points. To construct Delaunay Lofts, the number of samples has to be the same for each of the corresponding pairs of control lines in the top and bottom layers (see Section 3.5 for the definition of corresponding pairs of control lines).

3.5 Creation of Control Curves

The fourth step is really a standard Delaunay lofting process. We first identify corresponding pairs of control lines in the top and bottom layers. Let LT_i and LB_i denote two corresponding pairs of control lines at the top and bottom respectively. Then, we connect each Voronoi point obtained by sampling LT_i with another Voronoi point obtained by sampling LB_i with a curve as shown in

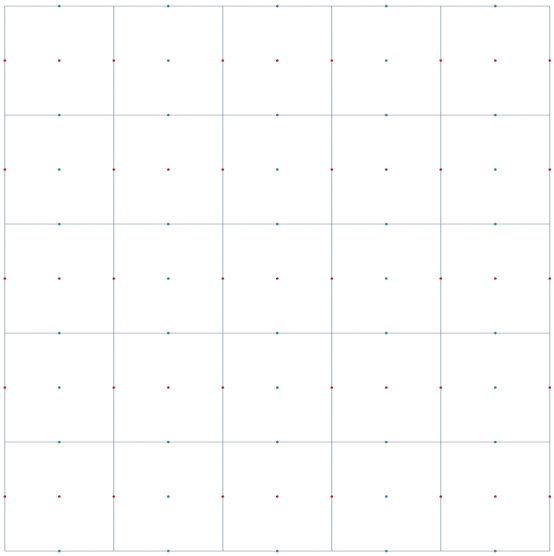

(a) Example of Sampling 3 Points on the top layer for the Plain Weave Pattern

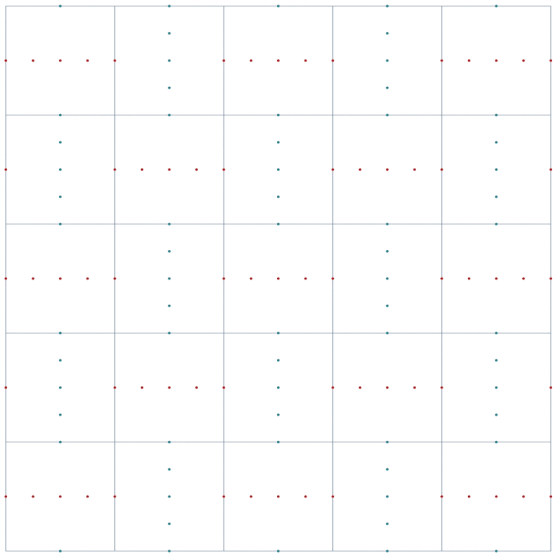

(b) Example of Sampling 5 Points on the top layer for the Plain Weave Pattern

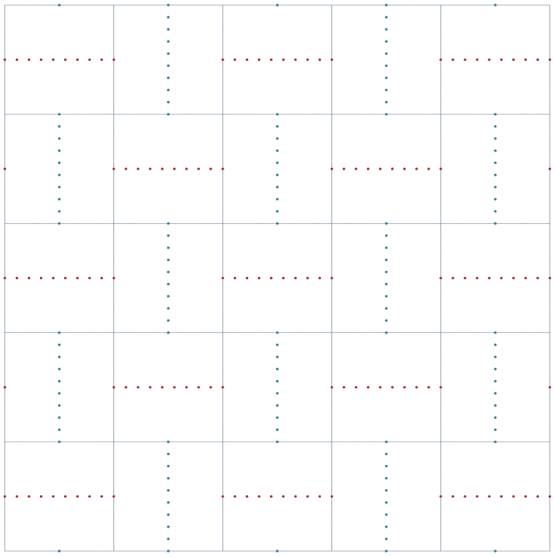

(c) Example of Sampling 10 Points on the top layer for the Plain Weave Pattern.

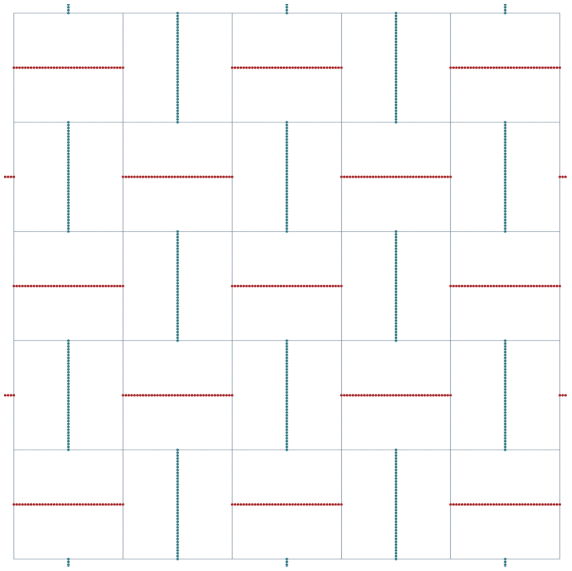

(d) Example of Sampling 20 Points on the top layer for the Plain Weave Pattern.

Figure 3.3: Step 3: Sampling the control lines with 3, 5, 10 and 20 Uniformly Distributed Points.

Figure 3.4. The shape of the curve also directly impacts the geometry and topology of woven tiles as discussed in Chapter 5.

Figure 3.4 shows an example of the control curve profile after creating control curves. In this example, the curves are obtained by rotating the control lines along the y-axis, such that 90 degrees of rotation occurs between the top and bottom layers and that the center of the rotation is the center of the axis that connects the two control lines. It should be noted that the control curves in the example shown in Figure 3.4 are not single curves, but rather a bundle of curves that when stitched together forms an overall control curve profile. In fact, we can view this bundle of curves not so much as a curve, but rather a surface.

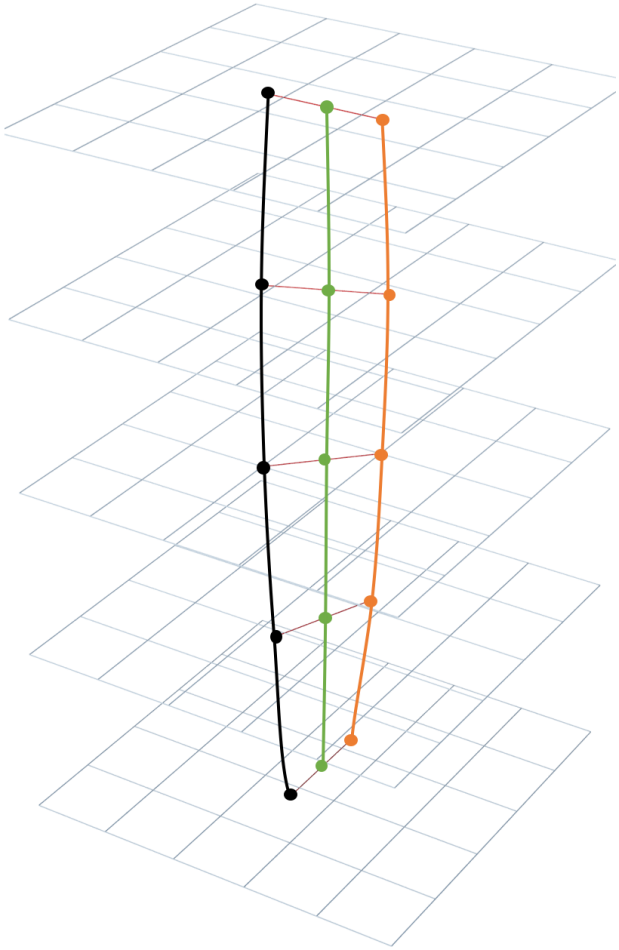

Figure 3.4: Step 4: Creation of Control Curve Profile Illustrated with 3 Sampled Points per Line

3.6 Subdivision of each Layer into Convex Polygons Using Voronoi Decomposition

The fifth step is subdivision of each layer into convex polygons. Before we introduce detailed analysis of this step, an introduction to the Voronoi Decomposition is necessary. Figure 3.5 shows the Voronoi Decomposition of a set of randomly placed points. The Voronoi algorithm is based on a distance function, with each site capturing the area that is closest to it relative to its' neighboring sites (points). As a result, a property of the Voronoi Decomposition is that we are guaranteed to generate a convex polygon for each cell.

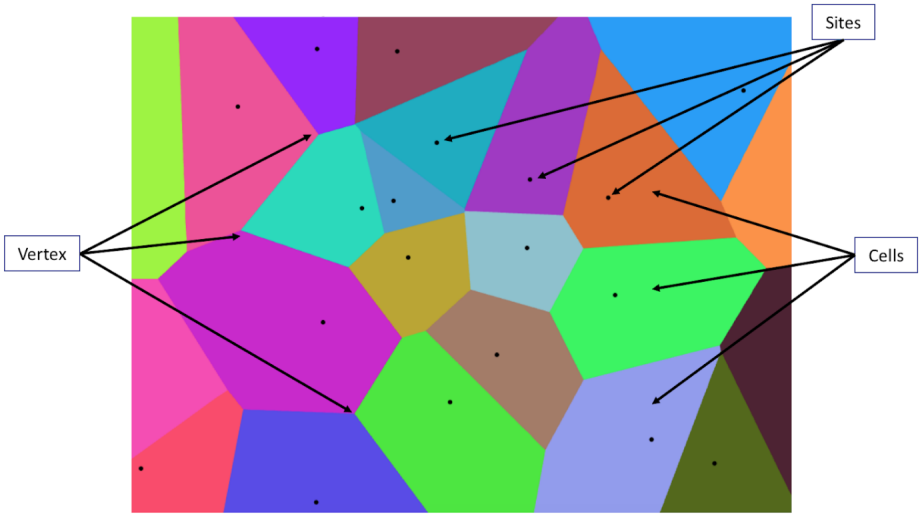

Figure 3.5: Voronoi Decomposition of Randomly Placed Points

During this step, the Voronoi Decomposition is applied on each layer. By adjusting the number and sampled position of the points on each line, a variety of convex polygons can be generated. This is further emphasized in Figure 3.6 for the top and bottom layers of the plain weave pattern. Figure 3.7 shows the entire visualization of decomposing each grid/plane into its Voronoi partitioning with 5 layers. In this scenario, Item 1 is the top layer, which is also shown in Figure 3.6a. Item 2 is the 2^{nd} layer. Item 3 is the middle, or 3^{rd} layer. Item 4 is the 4^{th} layer. Finally, Item 5 is the bottom layer, which is shown in Figure 3.6b.

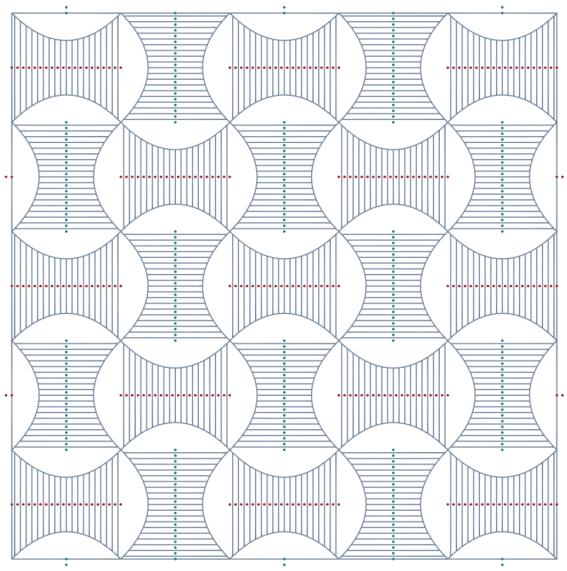

(a) Voronoi Decomposition of a Plain Weave Pattern at the Top Layer.

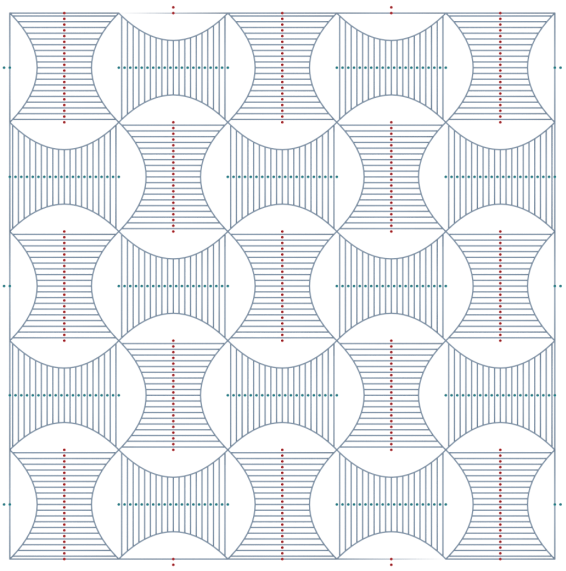

(b) Voronoi Decomposition of a Plain Weave Pattern at the Bottom Layer.

Figure 3.6: Step 5: Voronoi Decomposition Applied to a Single Layer, with 20 Uniformly Distributed Points per Line.

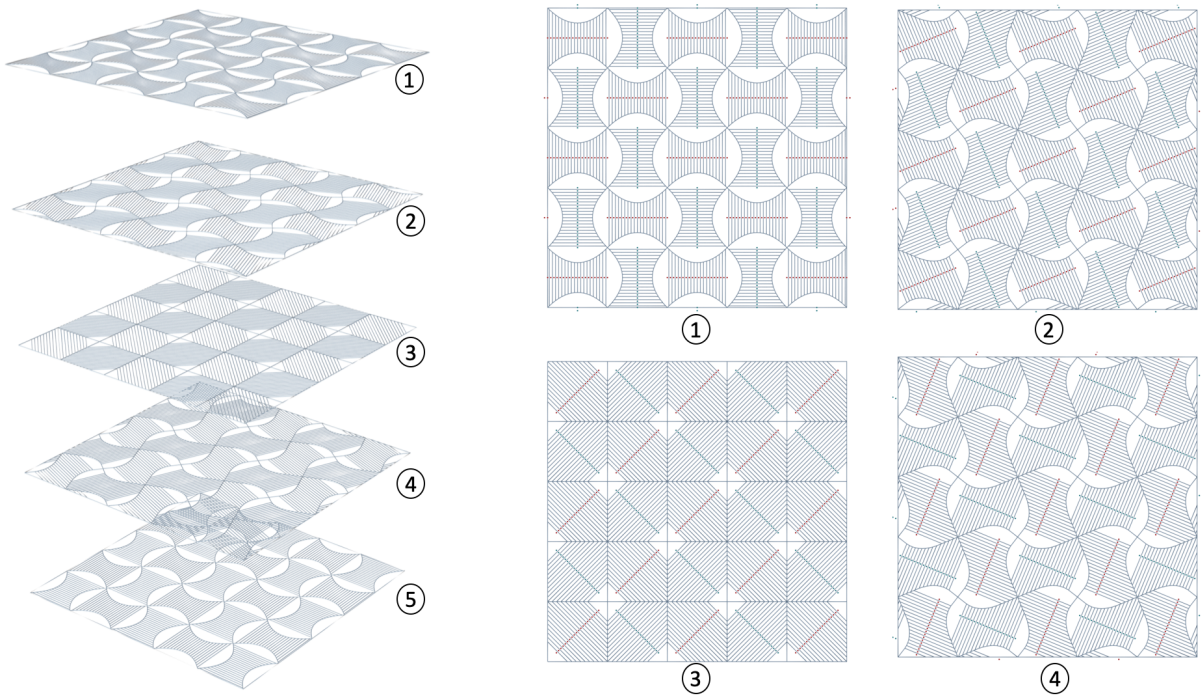

Figure 3.7: Step 5: Voronoi Decomposition applied to each layer. Item 1 is the top layer, also shown in Figure 3.6(a). Item 5 is the bottom layer (a 90° Rotation of Item 1), also shown in Figure 3.6(b).

3.7 Constructing Non-convex or Disconnected 2D as the Union of Convex Voronoi Polygons

The sixth step is constructing non-convex or disconnected 2D polygons as a union of the convex Voronoi polygons.

Before continuing on our process, an introduction to the conceptual process is necessary. First, let us assume that we have a countable number of 2D Voronoi sites in a given 2D plane. These sites are denoted by s_m, where $m = 0, 1, \ldots, M-1$. Second, assume that p_m denotes the convex polygon that is corresponding to s_m. Now, let us also assume that the Voronoi sites are decomposed into N disconnected sets denoted as G_n where $n = 0, 1, \ldots, N-1$. The sets must satisfy the two following conditions:

1. Disconnectivity Condition: For the Voronoi polygons in a grouped set, the intersection of the set must be an empty set. In other words:

$$G_k \cap G_l = \emptyset \quad \text{for all} \quad 0 < k, l < N-1 \quad \text{and} \quad k \neq l. \tag{3.1}$$

2. Curve Condition: For the Voronoi polygons in a grouped set, the valence of shared vertices in the set is never more than two. In other words;

$$p_k \cap p_l \cap p_j = \emptyset \quad \text{for any three different Voronoi points} \quad s_k, s_l, s_j \in \tag{3.2}$$

Then, non-convex and/or disconnected polygons are, then, defined as follows:

$$\mathcal{P}_n = \bigcup_{\forall s_m \in G_n} p_m$$

The two conditions 3.1 and 3.2 guarantee that the resulting structures approaches to curves. The area outlined in red in Figure 3.8 demonstrates an example of a valid grouped set by outlining the union shape in red for that particular set of grouped Voronoi sites grouped in G_n for the 3 Voronoi sites connected by the blue line.

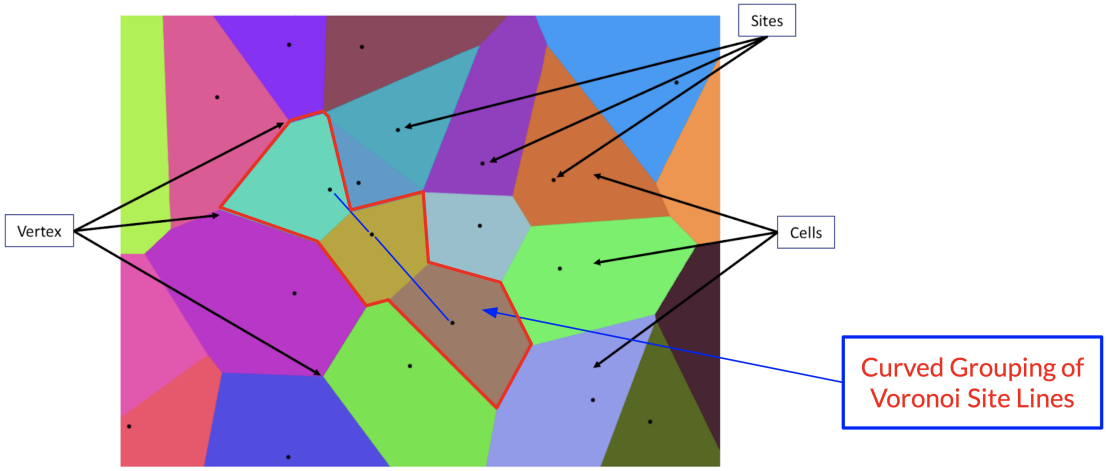

Figure 3.8: An example of curved grouping used to obtain the union for a subset of Voronoi polygons for a set of randomly placed points shown in Figure 3.5. In curved grouping, the valence of shared vertices is never more than two.

Now, we can explain our process of constructing non-convex or disconnected 2D polygons as a union of convex Voronoi polygons in terms of our plain weave pattern example. In this step, for each individual Voronoi site, the union of all of the convex polygons corresponding for each point on each sampled control line is taken and grouped together in a set. As a result, convex, non-convex, and disconnected polygons can be produced depending upon the layout of the Voronoi sites.

In Figure 3.9a, the resulting union shape is filled in red for a control line at the top layer, LT_i, because the cells all correspond to a site/point located on that particular control line. The union shape in blue is for another control line, LT_i, in an adjacent rectangular grid cell on the top layer. In Figure 3.9b, we highlight the resulting union shape filled in their respective colors to match the corresponding sampled points on LB_i at the bottom layer.

Figure 3.10 expands on the entire visualization from Figure 3.7 by using the corresponding colors to fill in the respective union shapes at each of the intermediate layers that are between the top and bottom layers using the same concept.

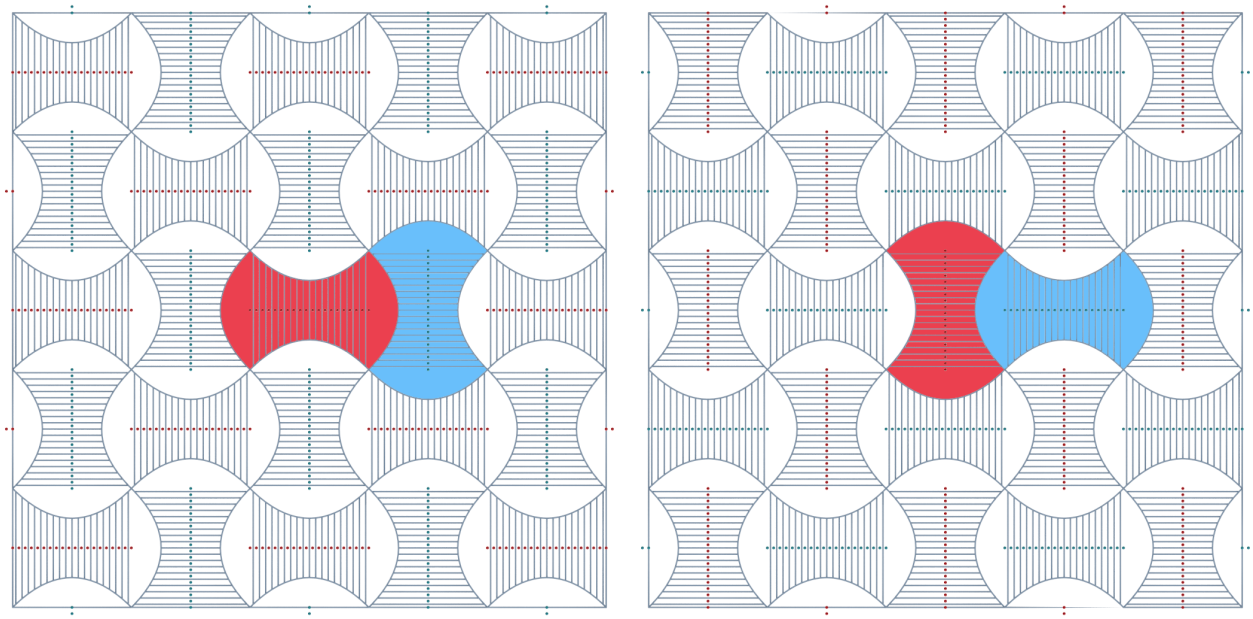

(a) Union at the Top Layer (b) Union at the Bottom Layer

Figure 3.9: Step 6: An example of 2D polygon construction as the union of Voronoi polygons at the top and bottom layers, with each Voronoi Cell corresponding to its respective Voronoi Site.

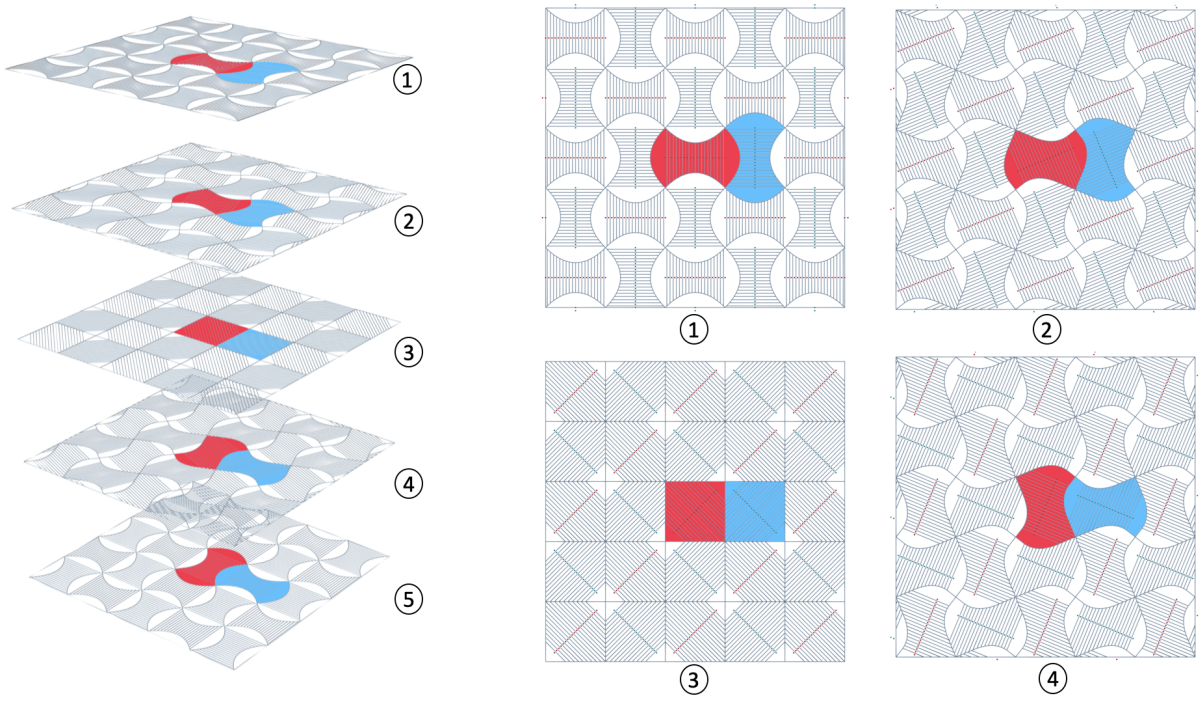

Figure 3.10: Step 6: Union of Voronoi Decomposition Applied to each Plane. Item 1 is the Top Layer, also shown in Figure 3.9(a). Item 5 is the Bottom Layer (a 90° Rotation of Item 1), also shown in Figure 3.9(b).

3.8 Obtain Extruded Polygons

The seventh step is to extrude the 2D polygons resulting from the union of Voronoi polygon cells. Up to this point, the polygons are only characterized on a grid, and are therefore considered infinitely thin. In this step, the overall pieces resulting from the union operation are extruded an amount to add thickness. This allows us to preview the shape of each individual layer.

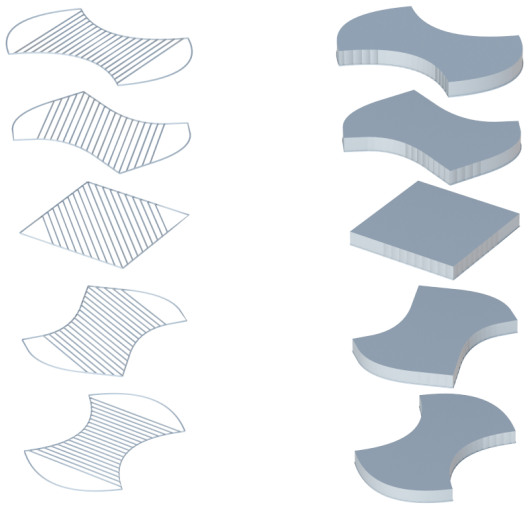

Figure 3.11: Step 7: Obtaining Extruded Polygons of 2D Voronoi Cells. The Union of 2D Polygons are on the Left, and the Extruded Polygons are on the Right. The Extrusion Depth Amount Determines the Connectivity of the Entire Structure.

Figure 3.11 shows a detailed exploded view of this step. In Figure 3.11 on the left, the union of the corresponding cells from the corresponding sampled line are shown. Then, in Figure 3.11 on the right, the 2D polygons are extruded a small amount. In this particular image, it is shown as an exploded view for clarity.

In order for the structure to transition together between the layers, there are various scenarios for the extrusion depth amount:

1. Extrusion depth amount is less than the distance between layers

2. Extrusion depth amount is greater than the distance between layers

3. Extrusion depth amount is equal to the distance between layers

For case 1, if the extrusion depth is less than the distance between layers, each polygon will become a separate piece, similar to what is shown in Figure 3.11. In case 2, if the extrusion depth is greater than the distance between each layer, the structure will become a single, connected entity, but there can potential be unclean modeling errors such as self-intersection within the overall structure. In case 3, if the extrusion depth amount equals the distance between each layer, the layers will stack on each other at the touching point and form a connected structure without any self-intersection.

3.9 Union of Extruded Polygons

The eighth, and final step of our process is to take the union of all extruded polygons. Once each individual layer is extruded, we will take the union of all extruded polygons in order to close the entire structure. Figure 3.12 shows this step. This allows us to view the entire, overall Woven tile structure. With more layers, the higher the resolution and the topology change of the geometry along the surface will become smoother due to the higher level of detail.

By observing the woven structure pattern, the structures are tilable and fit together. Houdini's powerful procedural modeling capabilities allowed us to be efficient with our computing resources by only having to focus on a single cell to apply the framework, and then repeat the structure throughout the scene. Houdini's Mantra renderer was used to render out still images of the structures.

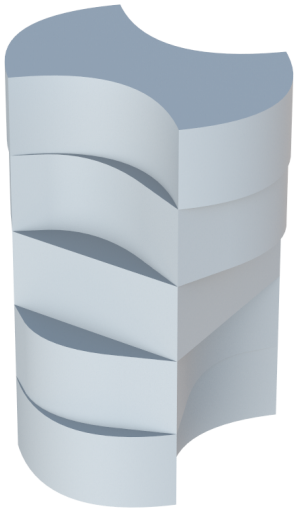

Figure 3.12: Step 8: Take the Union of the Extruded Polygons. The Extrusion Depth Amount is Set Equal to the Distance Between each Layer in order for each Polygon to Touch and Rest on Other Layers.

4.1 Software

We have implemented our procedural framework within SideFX's Houdini software. Houdini's node networks allow for the upstream manipulation of parameters. As a result, our framework allows the user to adjust various settings and rules in order to determine the final structure. Additionally, Houdini also implements the use of VEX code, "a high-performance expression language" that can be used in several applications [45]. One of the areas encompasses modeling, which provides the user with the ability to "manipulat[e] point attributes" [45].

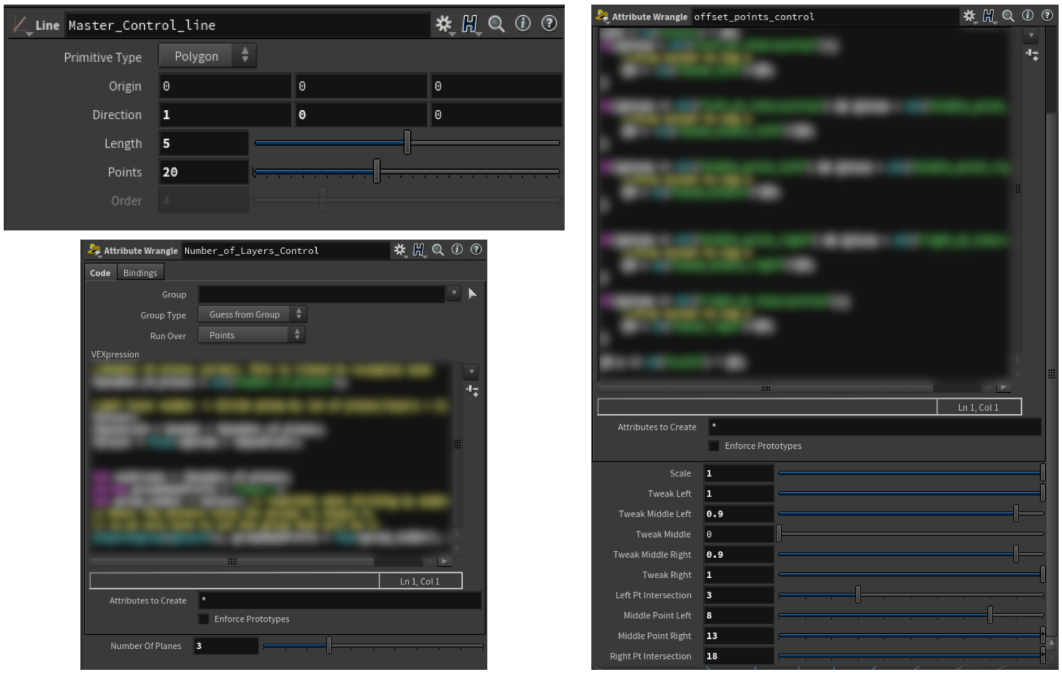

Figure 4.1: Some interfaces from our procedural workflow and examples of parameters used to modify variables in our control lines.

A powerful concept within Houdini is its customization for organizing and manipulating data, which allows the user to set procedural rules across the node network. When one value is changed,

the user can link that value to another parameter in the node network so that the system automatically updates. The end result is a highly flexible system that can adapt to user input.

4.2 Procedural System

4.2.1 Voronoi Site Guide Lines

With respect to the individual Voronoi Site Guide Lines (or control lines referred to in Chapter 3) themselves, our framework offers the following flexibility.

4.2.1.1 Number of Points on the Line

The user can adjust the total number of points on the line. This causes a change to the Voronoi Decomposition. A notable result is that once the number of points is greater than 8, the shapes generated are similar to geometric planar tesselation work by Miadragovivc [37].

4.2.1.2 Position of the Points on the Line

By default, the position of the points on the line are evenly divided, resulting in equal spacing between each individual point. In our workflow, the position of the points along the line can also be moved throughout the line according to user preferences. This feature is important in controlling the interaction of where the lines for the woven patterns potentially meet. If designed correctly, the Voronoi Decompositon can create a gap between the individual pieces/cells when taking the union. In Figure 4.3 below, part (c), notice how the middle cells are a little bit wider compared to its counterpart without the offset in Figure 4.2, part (e) above.

4.2.2 Design of the Control Curves

4.2.2.1 Rotation

By carefully designing the position of the Voronoi Sites, we can create interesting polygons by applying transformations to the Voronoi Site Guide Lines. One such example is rotating the lines about their center throughout the structure. Figure 4.4 shows the lines being rotated 90 degrees between the top and bottom layers. Each layer is evenly rotated using interpolation depending on the total number of layers. For clarity, only a 5 layer structure is shown.

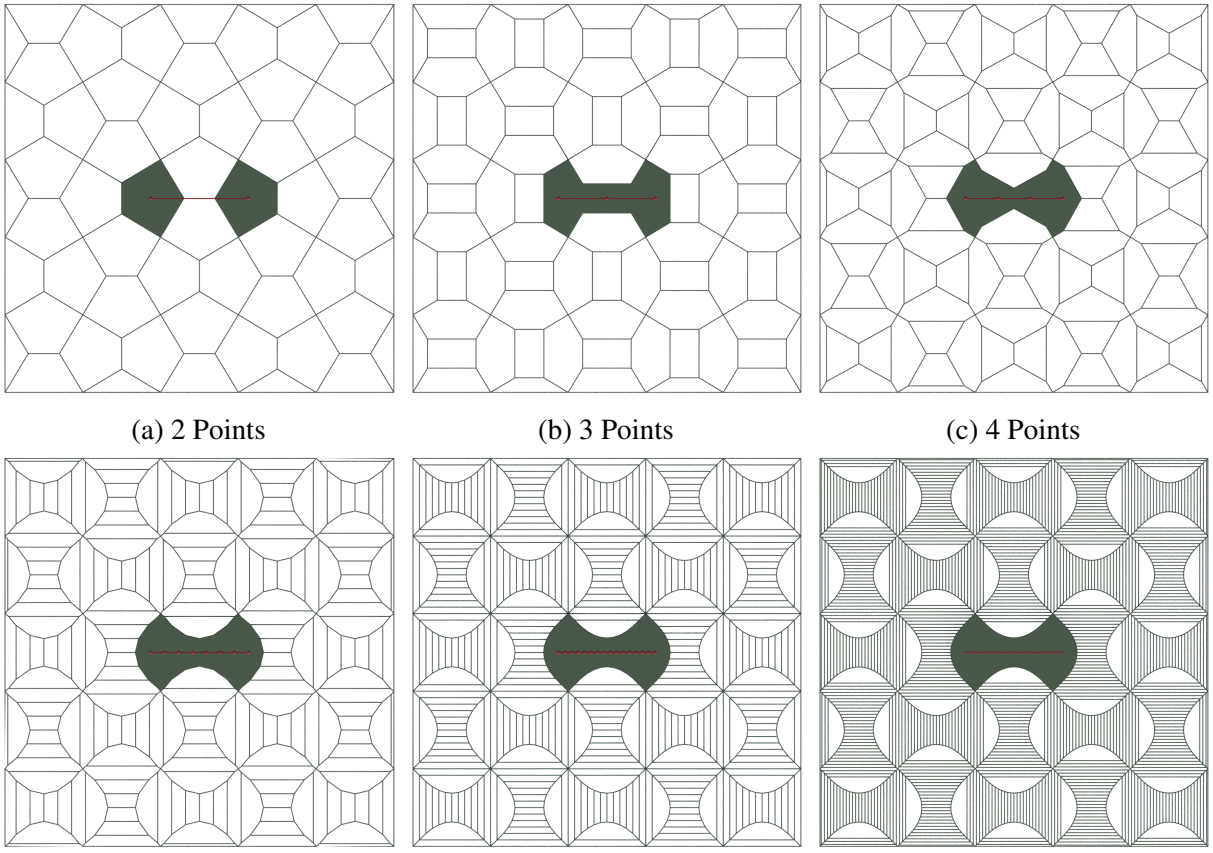

(a) 2 Points (b) 3 Points (c) 4 Points

(d) 8 Points (e) 16 Points (f) 32 Points

Figure 4.2: Adjusting the point density on the Voronoi Site Guide Lines.

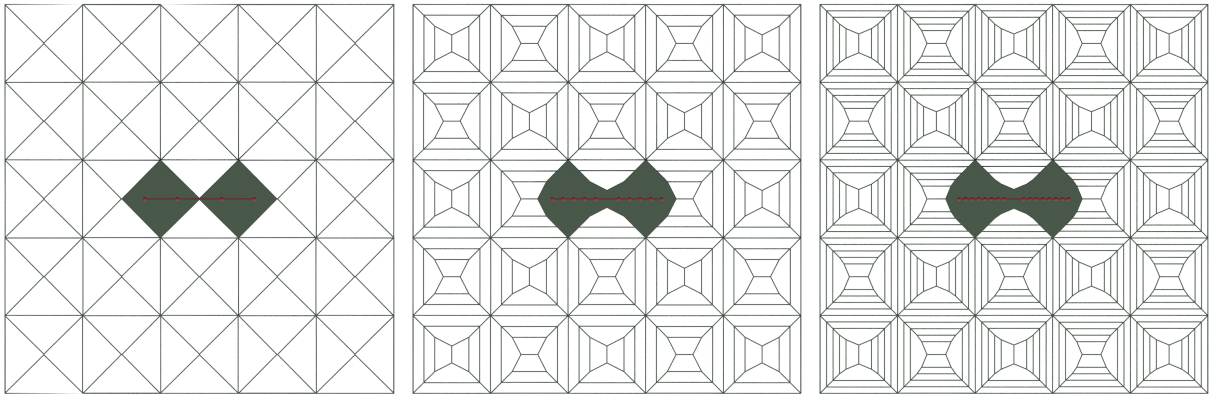

(a) 4 Points Offset (b) 10 Points Offset (c) 16 Points Offset

Figure 4.3: Adjusting the point position away from the center of the Voronoi Site Guide Lines.

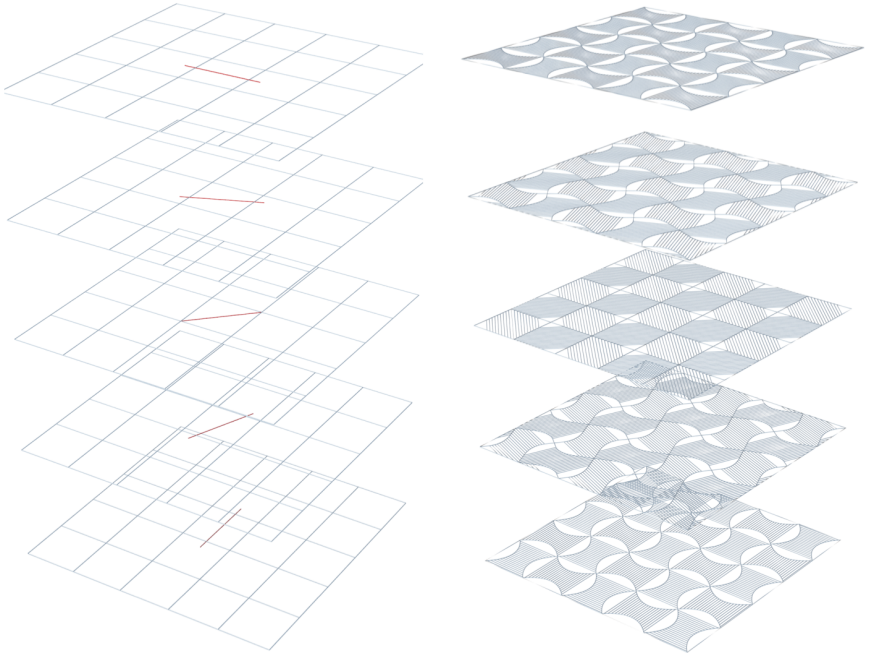

Figure 4.4: Example of rotating the control lines.

To help visualize how the Voronoi Site Guide Lines transform throughout the structure, Figure 4.5 shows how the Voronoi Site Guide Lines appear from the Top Orthographic viewport for a single woven pattern cell. The lines are rotated counter-clockwise.

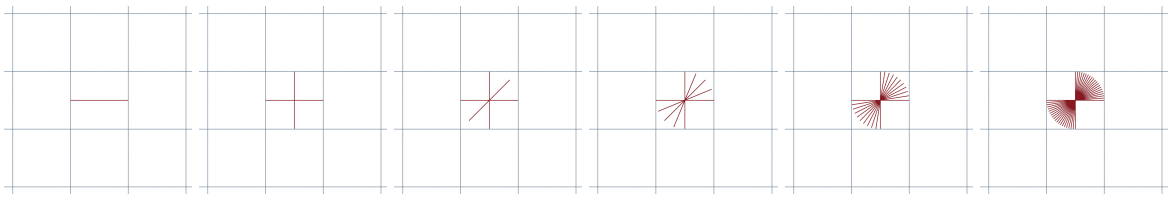

(a) 1 Layer - 0° Rotation (b) 2 Layers - 90° Rotation (c) 3 Layers - 45° Rotation (d) 5 Layers - 22.5° Rotation (e) 11 Layers - 9° Rotation (f) 21 Layers - 4.5° Rotation

Figure 4.5: Top orthographic view to see the rotation of control lines of a single plain weave rectangular grid cell.

Figure 4.6 shows how the Voronoi Site Guide Lines interact with each other as they are rotated on each layer down the structure. Both sets of Voronoi Site Guide Lines are rotated counter-

clockwise.

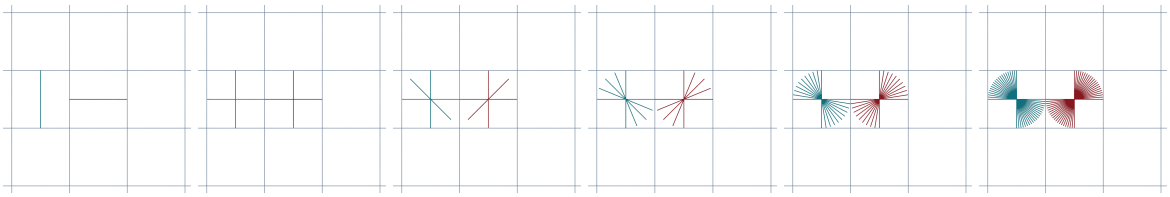

(a) 1 Layer - 0° Rotation (b) 2 Layers - 90° Rotation (c) 3 Layers - 45° Rotation (d) 5 Layers - 22.5° Rotation (e) 11 Layers - 9° Rotation (f) 21 Layers - 4.5° Rotation

Figure 4.6: Top orthographic view to see the rotation of control lines of a pair of plain weave rectuangular grid cells.

Figure 4.7 shows how the Voronoi Site Guide Lines interact when tiled across the entire grid space. This further emphasizes the unique symmetrical potential of the woven patterns. A notable characteristic is the negative space they create between the grid cells. Additionally, a cause of concern is the intersection of potential Voronoi Site Guide Lines depending on the length. This proposes an unexpected issue when taking the Union of the Voronoi cells per Site Line as the intersection causes holes in the union structure.

4.2.2.2 Scaling

When working with the basic plain woven pattern, careful attention must be paid to the intersection of the Voronoi Site Guide Lines. Depending upon the length of the Site Lines, as the counter-clockwise rotation about the center of each grid cells occur, they may intersect with an adjacent grid cell's Voronoi Site Line. When taking the union of the pieces, this causes some ambiguity as to which pieces should belong to which line. To avoid this issue, a solution is to scale the lines to force no intersection of the Site Lines.

Therefore, Figure 4.8 provides the geometric analysis to determine the intersection length threshold - the maximum Voronoi Site Line length to guarantee that intersections will not occur. By applying the Pythagorean Theorem for a square, we see:

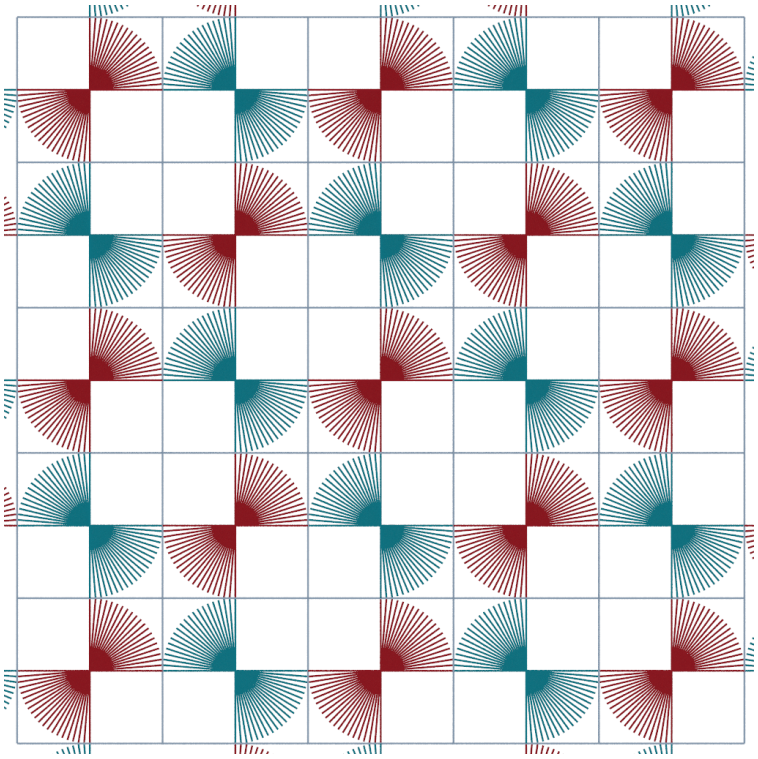

Figure 4.7: Entire grid space with rotated Voronoi Site Guide Lines.

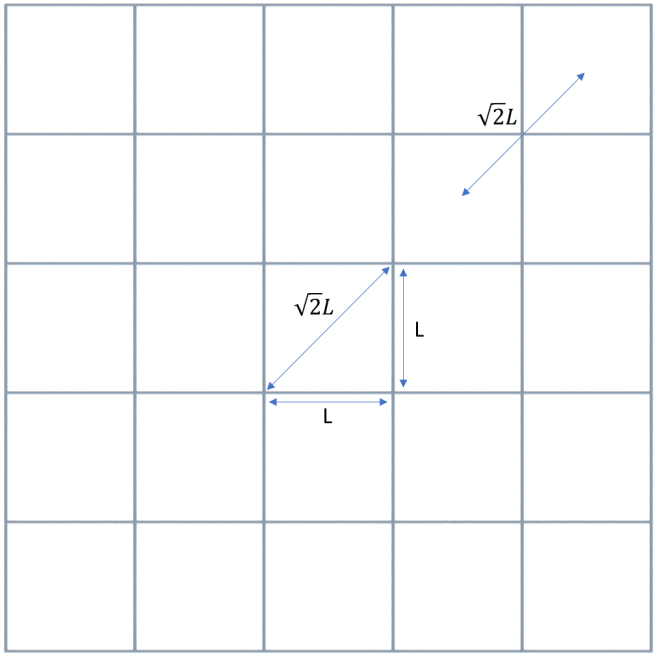

Figure 4.8: Geometry for determining the Intersection Length Threshold.

$$IntersectionThresholdLength = \sqrt{2}L$$

where L is the length of a unit grid cell within the rectangular grid space.

As long as the length of the Voronoi Site Guide Lines are less than this value, then no intersections will occur. If the length of the Voronoi Site Guide Lines are chosen to be greater than this value, there will be intersections and the user must decide on how to treat the intersections and union of pieces.

Our node network interface allows the user to customize the tapering of the Control Curve profile through a ramp interface - shown in Figure 4.9. The left side represents the scale of the lines at the top layer, and the right side represents the scale of the lines at the bottom layer. In this example, we are decreasing the scale, and thus length of the Voronoi Site Guide Lines towards the middle layer.

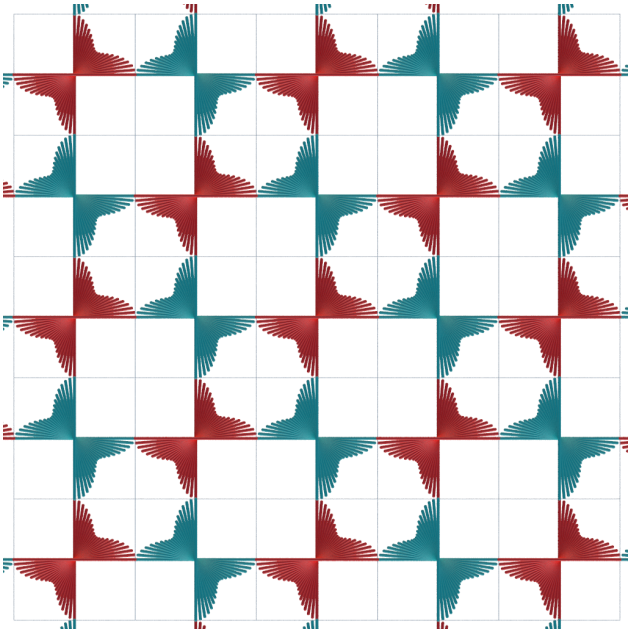

(a) Entire grid space with rotated and scaled Voronoi Site Guide Lines.

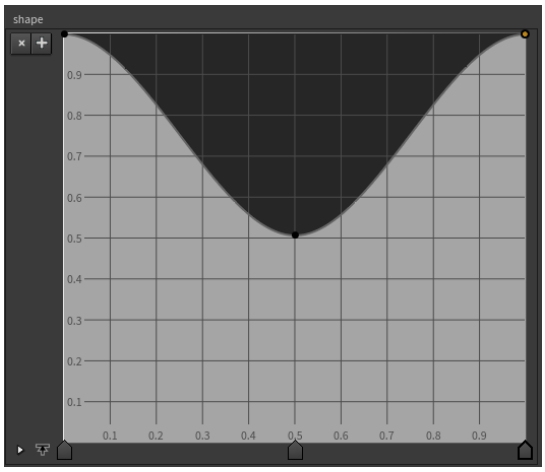

(b) User-controlled ramp profile to adjust the Voronoi Site line length scale.

Figure 4.9: Scaling the profile of the control curves.

Based upon the classification of conditions that may exist, the following two conditions are established in regards on how to handle the potential intersections of lines:

$$ControlCurveProfile = \begin{cases} Rotation, & \text{if } Length < \sqrt{2}L \\ Rotation + Scaling, & \text{if } Length \geq \sqrt{2}L \end{cases} \tag{4.1}$$

Going forward, we will consider Case 1 being the scenario when the Voronoi Site Line Length is less than the Unit Length of a Grid Cell. Case 2 is when the Voronoi Site Line Length is greater than or equal to the Unity Length of a Grid Cell.

4.2.3 3D Printing

Aspirations of 3D printing our structures were to provide both a visual aid and physically tangible product, study the interlocking features, confirm the tiling/space filling capabilities, and to help facilitate brainstorming ideas from mechanical perspectives such as structural potential and fluid flow.

5.1 Plain Woven Pattern

By using our subsequent procedural framework within the established rules, we were able to generate several Woven Structure based Delaunay Lofts. By controleling the parameters, we are able to quickly investigate how certain parameters affected the final resulting structure. Most importantly, we are able to control the resulting union shape on each layer by specifying and designing the Voronoi Decompositon.

In the following sections, our parameters were 20 points on each Voronoi Site Guide Line, with 41 layers throughout the structure. We believe that this combination of parameters provided the proper balance between computing time and detail within the results. The renders (created in Houdini using SideFX's Mantra renderer) are examples of the Delaunay Lofts resulting from the Plain Woven Pattern.

5.1.1 Case 1: Voronoi Site Guide Line Length < Intersection Threshold Length

The following is the layout of the Voronoi Site Guide Lines for Plain Woven Pattern, Case 1.

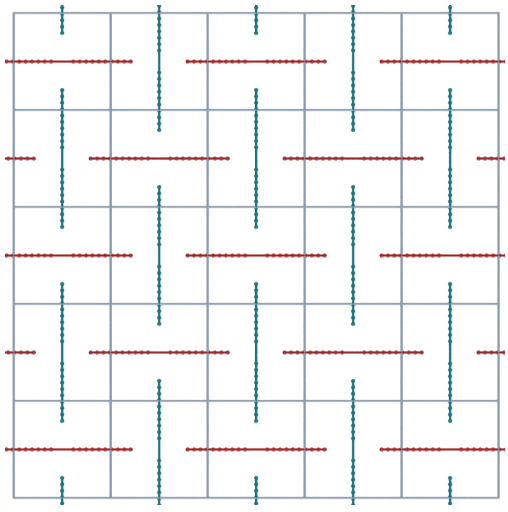

Figure 5.1: Case 1: Voronoi Site Guide Line Length < Intersection Threshold Length

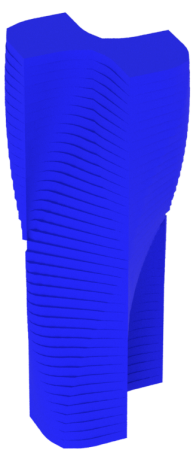

(a) Plain Woven Pattern Horizontal Line Delaunay Lofts

(b) Plain Woven Pattern Vertical Line Delaunay Loft

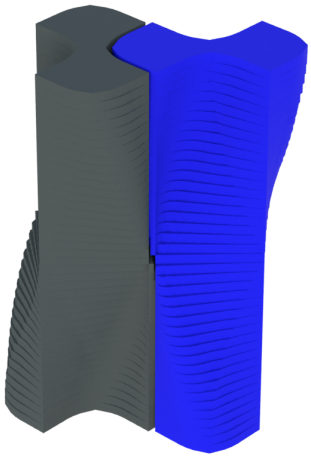

(c) Fitting the Pieces Together

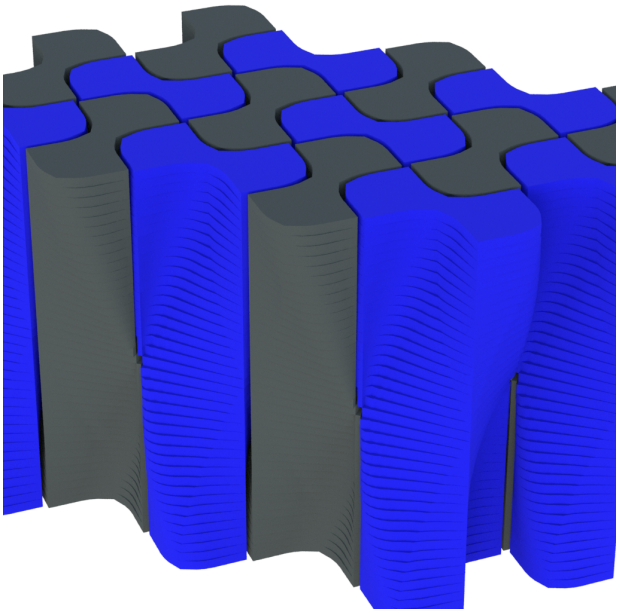

(d) Plain Woven Pattern Vertical Delaunay Lofts Tiled

Figure 5.2: Renders of Case 1: Plain Woven Pattern Delaunay Lofts

The resulting renders of the final structure generated from Case 1 for the Plain Woven Pattern Delaunay Lofts are shown in Figure 5.2. Overall, our method creates a structure similar to the

tessellations formed by Miadragovic's team [37]. Additionally, notice how the each individual structure fits together in the entire pattern.

5.1.2 Case 2: Voronoi Site Guide Line Length $\geq$ Intersection Threshold Length

The following is the layout of the Voronoi Site Guide Lines for Plain Woven Pattern, Case 2.

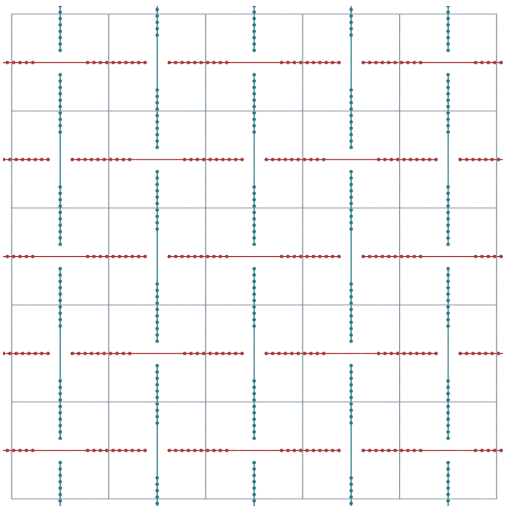

Figure 5.3: Case 2: Voronoi Site Guide Line Length $\geq$ Intersection Threshold Length

Since the intersection of Voronoi Site Guide Lines occur in Case 2 , a scaling rule was applied to the length of the Voronoi Site Guide Lines. The profile is similar to the inverted bell curve in Figure 4.9. As a result, the length of the lines decreases towards the middle layer. This guarantees that we get a clean quadrilateral at the middle layer. When the lines intersect, we see that when taking the union, while we get an interesting shape, the resulting unions would collide with each other when trying to fit together, and therefore the overall structures would not be tileable and space-filling.

The resulting renders of the final structure generated from Case 2 for the Plain Woven Pattern Delaunay Lofts are shown in Figure 5.5. Notice how the each individual structure fits together in the overall structure. Due to the gap, no only do these structures have a more peculiar topology,

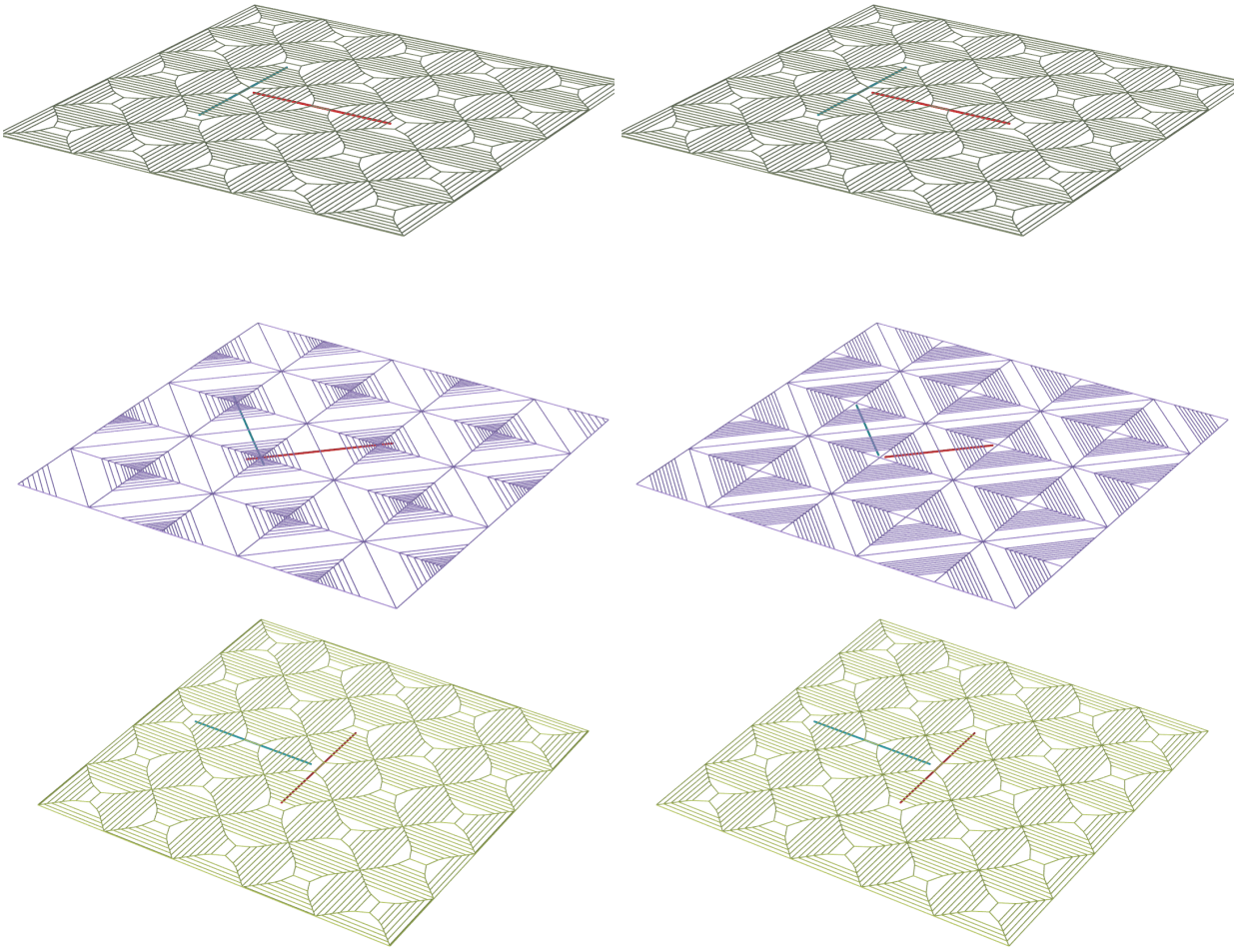

(a) No Scaling of Voronoi Site Guide Line Length

(b) Scaling of the Voronoi Site Guide Line Length towards the Middle Layer

Figure 5.4: Effect of Scaling on the Control Curve Profile

they also fit in a more unnatural way. Compared to Case 1, the interlocking mechanics of Case 2 create potentially greater mechanical strength.

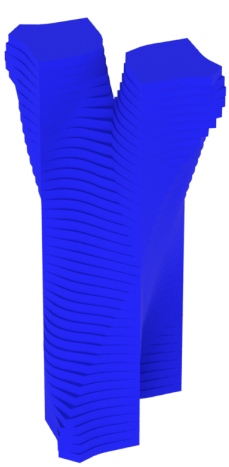

(a) Plain Woven Pattern Horizontal Line Delaunay Loft

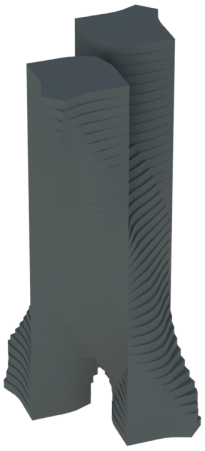

(b) Plain Woven Pattern Vertical Line Delaunay Loft

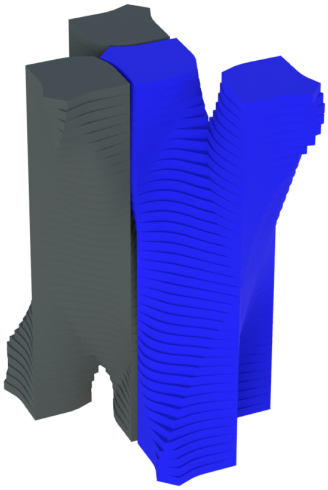

(c) Fitting the Pieces Together

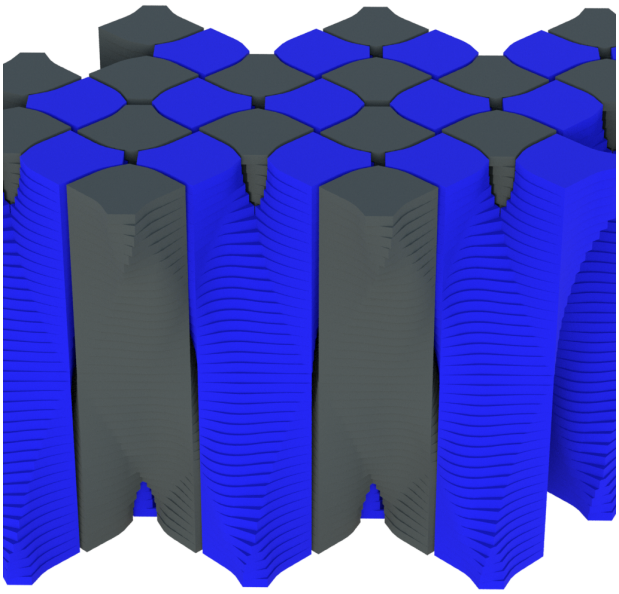

(d) Plain Woven Pattern Delaunay Lofts Tiled

Figure 5.5: Renders of Case 2: Plain Woven Pattern Delaunay Lofts

5.2 Twill Woven Pattern

5.2.1 Case 1: Voronoi Site Guide Line Length < Intersection Threshold Length

Figure 5.6 shows the layout of the Voronoi Site Guide Lines for the Twill Woven Pattern, Case 1. The Voronoi Site Guide Line length is less than the Intersection Threshold Length. Also, the entire grid was not filled in with the Twill Line Pattern to a)save on computation cost and b) the repetitive structure was already captured in fewer grid cells.

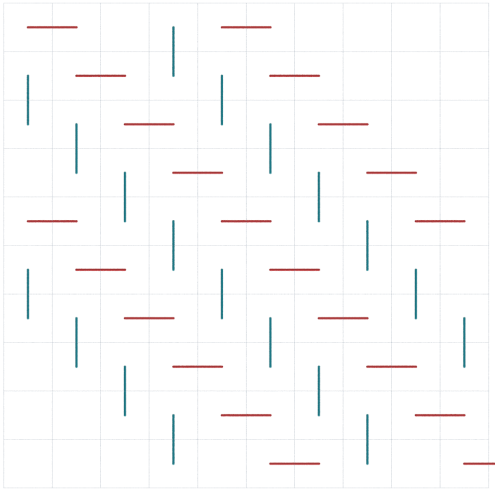

Figure 5.6: Case 1: Voronoi Site Guide Line Length < Intersection Threshold Length

The Voronoi Site Guide Lines were rotated a total of 90 degrees counter-clockwise throughout the layers to produce the resulting renders are shown in Figure 5.7.

5.2.2 Case 2: Voronoi Site Guide Line Length $\geq$ Intersection Threshold Length

Figure 5.8 shows the layout of the Voronoi Site Guide Lines for the Twill Woven Pattern, Case 2. The lines are noticeably extended towards the neighboring lines.

Without scaling applied, there was intersection at the middle layers. However, due to the layout of the lines, the overlap was only among the same structures (i.e. the vertical blue lines only intersected with its neighboring vertical blue line when both were rotated 45 degrees).

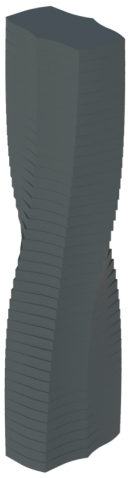

(a) Twill Woven Pattern Horizontal Line Delaunay Lofts

(b) Twill Woven Pattern Vertical Line Delaunay Loft

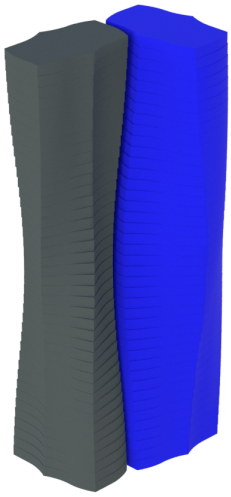

(c) Fitting the Pieces Together

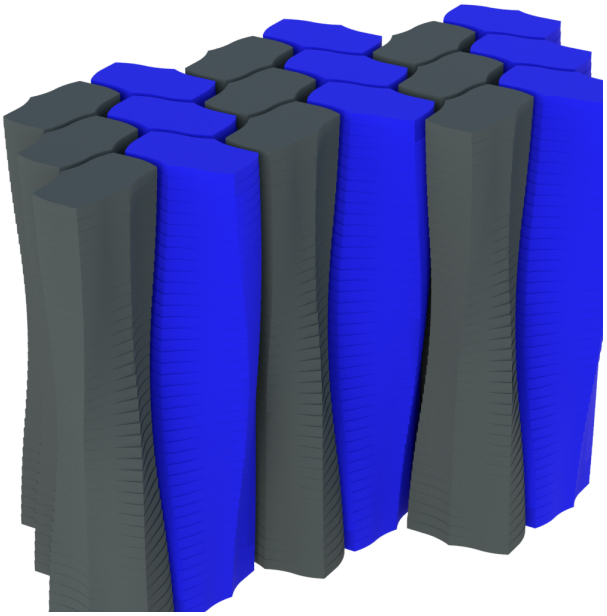

(d) Twill Woven Pattern Delaunay Lofts Tiled

Figure 5.7: Renders of Case 1: Twill Woven Pattern Delaunay Lofts

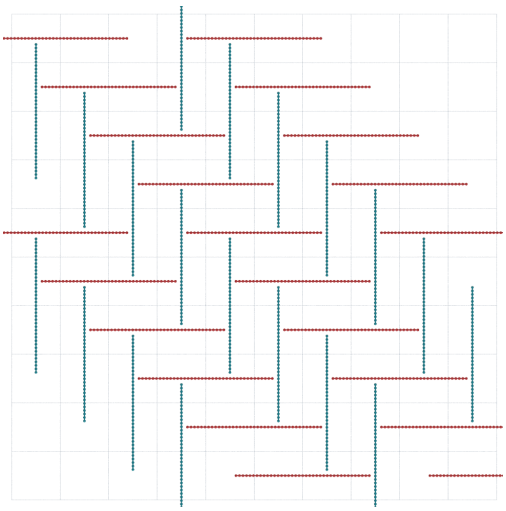

Figure 5.8: Case 2: Voronoi Site Guide Line Length $\geq$ Intersection Threshold Length

Therefore, a scaling function was applied to shorten the lines towards the middle. Figure 5.9 displays the renders. Due to the offset in the Twill pattern, we don't get a quadrilateral, but the scaling function guarantees that we get a clean convex or non-convex polygon at the middle layer.

5.2.2.1 Case 2 extended: Voronoi Site Guide Line Length $\geq$ Intersection Threshold Length

As previously mentioned, by finely tuning the point position where lines within the woven pattern intersect, a gap/hole can be created in the resulting layer when taking the union of the connected cells. For the Twill woven pattern, Figure 5.10 shows an application of this idea. Our method provides a way to not only create completely joined pieces, but also provides a design method to create disconnected pieces within the overall structure. Figure 5.11 displays the renders.

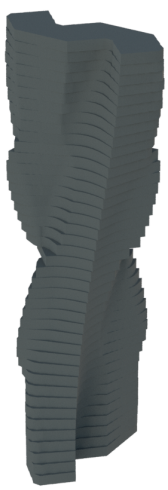

(a) Twill Woven Pattern Horizontal Line Delaunay Lofts

(b) Twill Woven Pattern Vertical Line Delaunay Loft

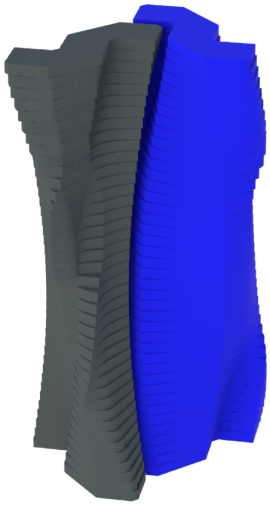

(c) Fitting the Pieces Together

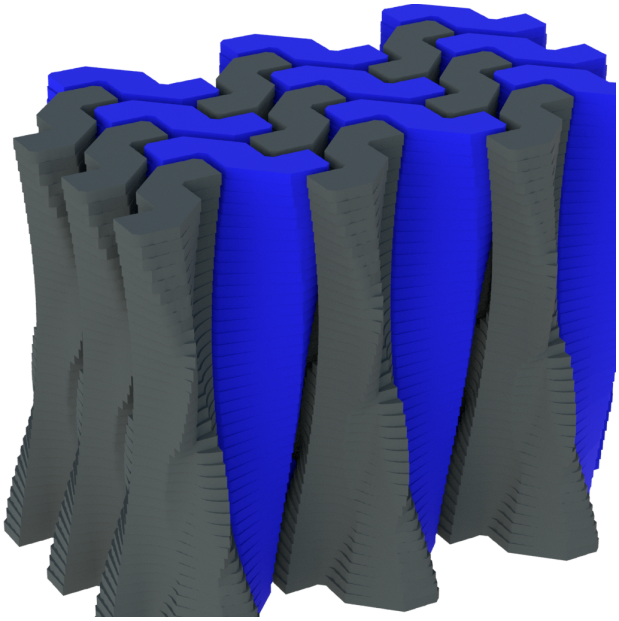

(d) Twill Woven Pattern Delaunay Lofts Tiled

Figure 5.9: Renders of Case 2: Twill Woven Pattern Delaunay Lofts

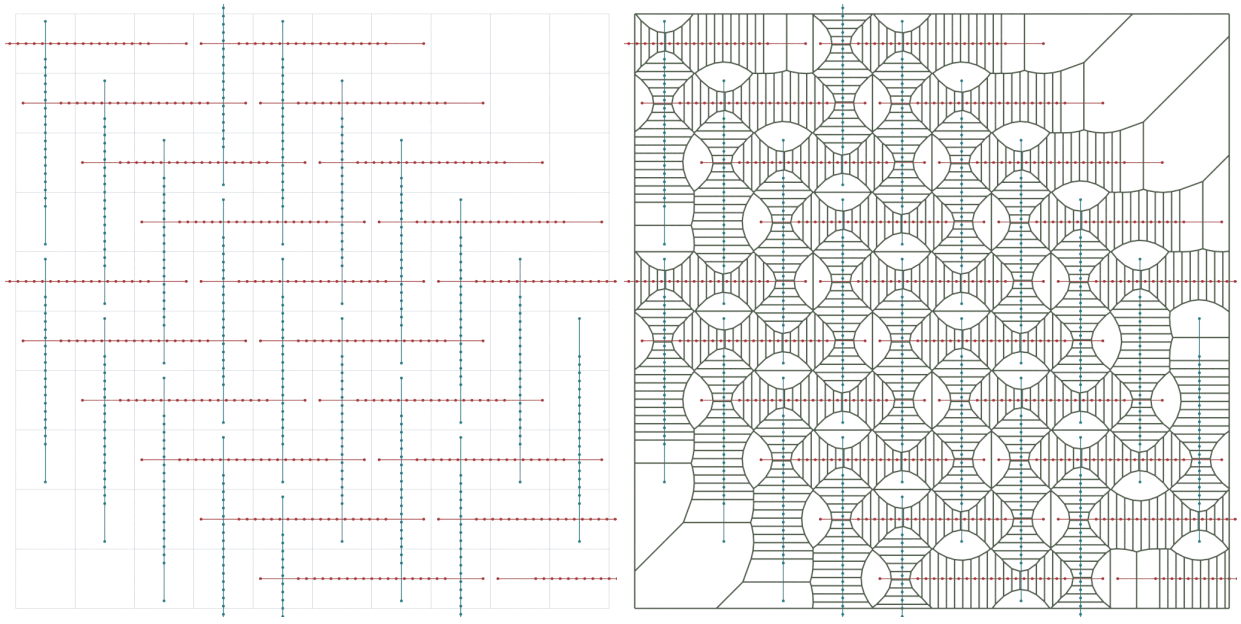

(a) Case 2 Extended: Voronoi Site Guide Line Layout

(b) Twill Woven Pattern Extended Voronoi Decomposition of Top Layer

Figure 5.10: Input of Case 2 Extended: Twill Woven Pattern Delaunay Lofts

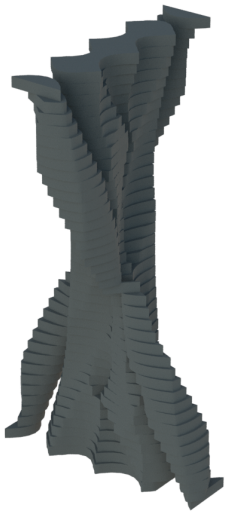

(a) Twill Woven Pattern Extended Horizontal Line Delaunay Lofts

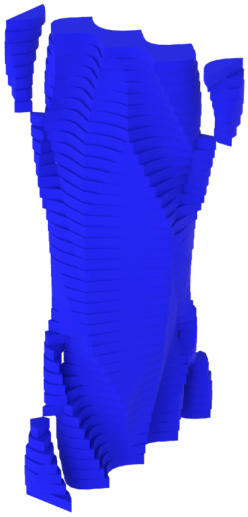

(b) Twill Woven Pattern Extended Vertical Line Delaunay Loft

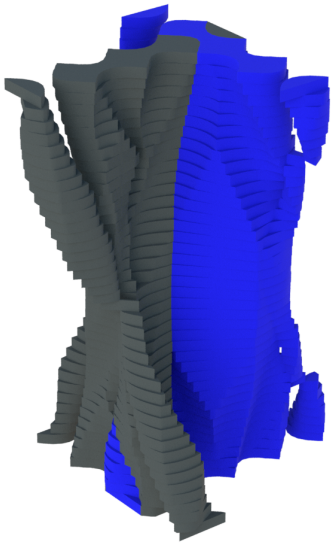

(c) Fitting the Pieces Together

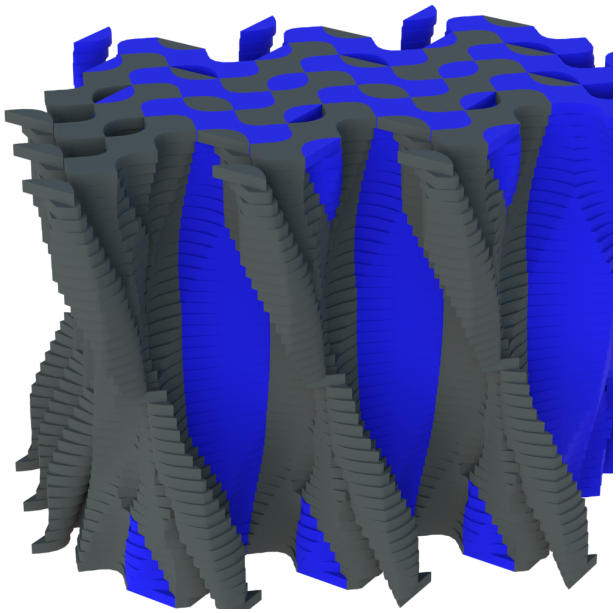

(d) Twill Woven Pattern Extended Delaunay Lofts Tiled

Figure 5.11: Renders of Case 2 Extended: Twill Woven Pattern Delaunay Lofts

6. CONCLUSION AND FUTURE WORK

6.1 Conclusion

This paper presents a procedural framework for the creation of Woven Structures as the result of taking the union of several Delaunay Lofts. As this method can reproduce several iterations of different structures, it is a powerful and useful algorithm for developing complex structures which can lead to various mechanical, architectural, and artistic implementations.

6.2 Future Work

While our procedural framework and algorithm is applicable to limitless Voronoi Site inputs, we focused strictly on a few cases of Woven Structures. Therefore, this work can be extended upon to include variations on other patterns and symmetrical designs. Further examples of woven structures include the Satin weave pattern, Japanese Bamboo Weave, or Basket weave pattern. Graphical designs outside of the textile and architecture industry are also possible sources of inspiration and exploration for the Voronoi Site points.

Furthermore, we only investigated constant/uniform transformations when defining the Control Curve profile. Variations on the rate of transformation applied may yield further complex structures. For instance, an option is to have non-uniform rotation where the rate of rotation fluctuates. Or, the directions of rotation can be changed depending on if the Voronoi Site Line is vertical or horizontal, rather than always being counter-clockwise.

Within Houdini, the structure of the framework could be reworked to incorporate more VEX code during the process. As VEX is multi-threaded, it typically runs faster and more efficiently than packaged SOPs, which could allow the process to cook more quickly when working with high resolution magnitudes of geometry [45]. Additionally, there is some needed manual editing when sorting the union of the grouped Voronoi Cells. While this is not a difficult task, it is probably beneficial in terms of turn-around time to have the software group the pieces rather than by the user manually selecting them, especially as the number of layers exponentially increases.

In terms of mechanical properties, further FEA (Finite Element Analysis) should be applied to the shapes to observe the stress distribution on the structures. The interlocking and tilable properties already provide promising observations for geometric strength, and optimal material properties other than 3D resin should be investigated. Furthermore, fluid dynamics and heat transfer studies could provide additional avenues for mechanical applications.

With respect to 3D printing, as one of the most intriguing characteristics of the Delaunay Loft's structure is in it's tiling capabilities, these pieces would be printed at a relatively small scale, but in mass quantities. Therefore, minimizing the production costs is a factor in determining 3D printing settings. One way to reduce costs would be to hollow out the structure in order to reduce the amount of material required, thus reducing the overall monetary cost. Additionally, the prints could also be textured or painted in a more creative manner to add visual interest during assembly, such as a color-coded puzzle.

REFERENCES

[1] Ergun Akleman, Jianer Chen, Qing Xing, and Jonathan L Gross. Cyclic plain-weaving on polygonal mesh surfaces with graph rotation systems. In *ACM Transactions on Graphics (TOG)*, volume 28, page 78. ACM, 2009.

[2] Kinney George Allison. Process for forming non-woven filamentary structures from fiber-forming synthetic organic polymers, August 29 1967. US Patent 3,338,992.

[3] Santiago Alvarez. The gyrobifastigium, not an uncommon shape in chemistry. *Coordination Chemistry Reviews*, 350:3–13, 2017.

[4] Attila Balogh, Balázs Farkas, Kornél Faragó, Attila Farkas, István Wagner, Ivo Van Assche, Geert Verreck, Zsombor K Nagy, and Gyoergy Marosi. Melt-blown and electrospun drug-loaded polymer fiber mats for dissolution enhancement: A comparative study. *Journal of pharmaceutical sciences*, 104(5):1767–1776, 2015.

[5] Nehemiah H. Brewster. Sheet material and method of making the same, October 30 1934. US Patent 1,978,620.

[6] MS Casper. *Nonwoven Textiles*. Noyes Data Corporation, 1975.

[7] Yen-Lin Chen, Ergun Akleman, Jianer Chen, and Qing Xing. Designing biaxial textile weaving patterns. *Hyperseeing: Special Issue on ISAMA'2010*, 6(2), 2010.

[8] C.R.J. Clapham. When a fabric hangs together. *Bulletin of the London Mathematics Society*, 12:161–164, 1980.

[9] C.R.J. Clapham. The bipartite tournament associated with a fabric. *Discrete Mathematics*, 57:195–197, 1985.

[10] Edward L. Clayton, James C. Draper, and Jesse H. Plummer. Method for producing non-woven glass fabric, March 22 1955. US Patent 2,704,734.

[11] PT Curtis and BB Moore. A comparison of the fatigue performance of woven and non-woven cfrp laminates in reversed axial loading. *International journal of fatigue*, 9(2):67–78, 1987.

[12] C. Delaney. When a fabric hangs together. *Ars Combinatoria*, 15:71–70, 1984.

[13] Mario Deuss, Daniele Panozzo, Emily Whiting, Yang Liu, Philippe Block, Olga Sorkine-Hornung, and Mark Pauly. Assembling self-supporting structures. *ACM Trans. Graph.*, 33(6):214:1–214:10, November 2014.

[14] Eugene J Dupre, Howard L Hoover, and Walter J Rankin. Low density open non-woven fibrous abrasive article, November 1 1960. US Patent 2,958,593.

[15] T. Enns. An efficient algorithm determining when a fabric hangs together. *Geometriae Dedicata*, 15:259–260, 1984.

[16] Giuseppe Fallacara. Toward a stereotomic design: Experimental constructions and didactic experiences. In *Proceedings of the Third International Congress on Construction History*, page 553, 2009.

[17] Martin Gardner. *Sixth book of mathematical games from Scientific American*. WH Freeman San Francisco, 1971.

[18] Michael Goldberg. The space-filling pentahedra. *Journal of Combinatorial Theory, Series A*, 13(3):437–443, 1972.

[19] Michael Goldberg. Convex polyhedral space-fillers of more than twelve faces. *Geometriae Dedicata*, 8(4):491–500, 1979.

[20] Michael Goldberg. On the space-filling enneahedra. *Geometriae Dedicata*, 12(3):297–306, 1982.

[21] Pedro Gómez-Gálvez, Pablo Vicente-Munuera, Antonio Tagua, Cristina Forja, Ana M Castro, Marta Letrán, Andrea Valencia-Expósito, Clara Grima, Marina Bermúdez-Gallardo, Ós-

car Serrano-Pérez-Higueras, et al. Scutoids are a geometrical solution to three-dimensional packing of epithelia. *Nature communications*, 9(1):2960, 2018.

[22] Boynton Graham. Non-woven sheet material, October 2 1956. US Patent 2,765,247.

[23] R. E. Griswold. Color complementation, part 1: Color-alternate weaves. Web Technical Report, Computer Science Department, University of Arizona, 2004.

[24] R. E. Griswold. From drawdown to draft - a programmer's view. Web Technical Report, Computer Science Department, University of Arizona, 2004.

[25] R. E. Griswold. When a fabric hangs together (or doesn't). Web Technical Report, Computer Science Department, University of Arizona, 2004.

[26] B. Grunbaum and G. Shephard. Satins and twills: an introduction to the geometry of fabrics. *Mathematics Magazine*, 53:139–161, 1980.

[27] B. Grunbaum and G. Shephard. A catalogue of isonemal fabrics. *Annals of the New York Academy of Sciences*, 440:279–298, 1985.

[28] B. Grunbaum and G. Shephard. An extension to the catalogue of isonemal fabrics. *Discrete Mathematics*, 60:155–192, 1986.

[29] B. Grunbaum and G. Shephard. Isonemal fabrics. *American Mathematical Monthly*, 95:5–30, 1988.

[30] Branko Grünbaum and Geoffrey C Shephard. Tilings with congruent tiles. *Bulletin of the American Mathematical Society*, 3(3):951–973, 1980.

[31] Hisao Honda. Description of cellular patterns by dirichlet domains: The two-dimensional case. *Journal of Theoretical Biology*, 72(3):523 – 543, 1978.

[32] Norman W Johnson. Convex polyhedra with regular faces. *Canadian Journal of Mathematics*, 18:169–200, 1966.

[33] Craig S. Kaplan. Voronoi diagrams and ornamental design. In *in The First Annual Symposium of the International Society for the Arts, Mathematics, and Architecture*, pages 277–283, 2000.

[34] Martin Kilian, Davide Pellis, Johannes Wallner, and Helmut Pottmann. Material-minimizing forms and structures. *ACM Trans. Graphics*, 36(6):article 173, 2017. Proc. SIGGRAPH Asia.

[35] Arthur L Loeb. Space-filling polyhedra. In *Space Structures*, pages 127–132. Springer, 1991.

[36] Ira Miadragovič Vella, Toni Kotnik, et al. Stereotomy, an early example of a material system. In *eCAADe*, 2017.

[37] Ira Miadragovič Vella, Toni Kotnik, Aulikki Herneoja, Toni Österlund, Pia Markkanen, et al. Geometric versatility of abeille vault. *eCAADe 2016*, 2016.

[38] Luis Pérez-Lombard, José Ortiz, and Christine Pout. A review on buildings energy consumption information. *Energy and buildings*, 40(3):394–398, 2008.

[39] Crosley Powel. Method of making laminated structures, March 18 1947. US Patent 2,417,586.

[40] AT Purdy. Developments in non-woven fabrics. *Textile Progress*, 12(4):1–86, 1983.

[41] Michaël Rao. Exhaustive search of convex pentagons which tile the plane. arXiv preprint arXiv:1708.00274, 2017.

[42] R. L. Roth. The symmetry groups of periodic isonemal fabrics. *Geometriae Dedicata, Springer Netherlands*, 48(2):191–210, 1993.

[43] Christian Schumacher, Steve Marschner, Markus Cross, and Bernhard Thomaszewski. Mechanical characterization of structured sheet materials. *ACM Trans. Graph.*, 37(4):148:1–148:15, July 2018.

[44] Hijung V. Shin, Christopher F. Porst, Etienne Vouga, John Ochsendorf, and Frédo Durand. Reconciling elastic and equilibrium methods for static analysis. *ACM Trans. Graph.*, 35(2):13:1–13:16, February 2016.

[45] SideFX Software. Vex. http://www.sidefx.com/docs/houdini/vex/index.html, 2019. Accessed: 2018-07-11.

[46] Sai Ganesh Subramanian, Mathew Eng, Vinayak R Krishnamurthy, and Ergun Akleman. Delaunay lofts: A biologically inspired approach for modeling space filling modular structures. *Computers & Graphics*, 2019.

[47] R.S.D. Thomas. Isonemal prefabrics with only parallel axes of symmetry. *Discrete Mathematics*, 309(9):2696–2711, 2009.

[48] R.S.D. Thomas. Isonemal prefabrics with perpendicular axes of symmetry. *Discrete Mathematics*, 309(9):2696–2711, 2009.

[49] R.S.D. Thomas. Isonemal prefabrics with no axis of symmetry. *Discrete Mathematics*, 310:1307–1324, 2010.

[50] Emily Whiting, John Ochsendorf, and Frédo Durand. Procedural modeling of structurally-sound masonry buildings. *ACM Trans. Graph.*, 28(5):112:1–112:9, December 2009.

[51] Emily Whiting, Hijung Shin, Robert Wang, John Ochsendorf, and Frédo Durand. Structural optimization of 3d masonry buildings. *ACM Trans. Graph.*, 31(6):159:1–159:11, November 2012.

[52] Robert Williams. *The geometrical foundation of natural structure: A source book of design*. Dover New York, 1979.

[53] Robert Edward Williams. Space-filling polyhedron: its relation to aggregates of soap bubbles, plant cells, and metal crystallites. *Science*, 161(3838):276–277, 1968.

[54] B. Zelinka. Isonemality and mononemality of woven fabrics. *Applications of Mathematics*, 3:194–198, 1983.

[55] B. Zelinka. Symmetries of woven fabrics. *Applications of Mathematics*, 29(1):14–22, 1984.